CX

CASD-NAS-75-030

BOSCH CO_2 REDUCTION SYSTEM DEVELOPMENT

INTERIM REPORT NO. 3

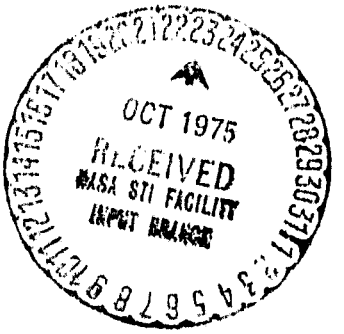

GENERAL DYNAMICS
Convair Division

Page intentionally left blank

TABLE OF CONTENTS

TABLE OF CONTENTS (Cont'd)

LIST OF FIGURES

LIST OF TABLES

SUMMARY

Significant advances in CO_2 reduction unit technology, principally through a major configuration change, were achieved during this contract period. Notable features of the new configuration are low-temperature reactor seals, a heat exchanger of simple geometry and high effectiveness, and improved thermal insulation. A unit of this configuration has been developed and operated for more than 2300 hours.

The fundamental concept of the cold-seal reactor is that components originating in the hot region are extended far enough in the direction of heat transfer to ambient that the thermal resistance due to path length reduces heat loss and outboard temperatures to acceptable values and allows use of elastomeric seals. Design of this unit is such that the cartridge is completely exposed and readily replaceable when the enclosing shell is lifted. Every surface and passage of the reactor assembly is readily exposed for inspection without damaging any component. Sealing of the vacuum insulation jacket is simplified so that high vacuum and high insulation performance are easily maintained.

The new configuration allows a relatively simple concentric shell recuperative heat exchanger design which operates at approximately 95 percent temperature effectiveness and makes a significant contribution to the power reduction effort. All heat exchanger surfaces can be exposed for inspection in the matter of a few minutes.

Operating experience with this unit has generated considerable information concerning the influence of reactor temperature, pressure, and recycle gas composition on power consumption. In general, precise control is not required since power consumption is not very sensitive to moderate variations of these parameters near their optimum values. Two process rate control modes are quite effective in minimizing power for a specific motor/compressor combination. Both regulate the recycle flow rate to match the process demand. The compressor bypass mode, because of its simplicity, is preferred if the design process load is relatively constant so the parasitic power can be minimized. The relatively complex variable compressor speed mode might be justified if the unit were required to respond to large variations in process load. Catalyst conditioning, support, and packing pattern developments have assured consistent starts, reduced energy consumption, and extended cartridge life. Four and five-man levels of operation have been maintained with overall power input values of 50 to 60 watts per man. It is estimated that an improvement of at least 15 percent could be achieved through design refinements with moderate engineering effort.

Material exposure tests and a study of the thermodynamic stabilities of metal carbides have to some extent clarified the problems involved when structural materials are exposed to the Bosch reaction environment, but no major breakthrough in this area has been made. Effective surface treatments to inhibit catalytic action have been devised but continued exposure will be required to establish their long-term efficacy.

1.0 INTRODUCTION

The cost of maintaining a metabolic oxygen supply for extended-duration manned space missions can be minimized by reclaiming oxygen from the metabolic carbon dioxide. The feasibility of using the Bosch reaction to reduce the carbon dioxide has been demonstrated previously. The main objective of this contract has been to develop and demonstrate Bosch CO_2 reduction unit refinements.

The reduction unit catalytically reacts CO_2 and H_2 to form water and solid carbon. The water is subsequently electrolyzed to provide metabolic oxygen and the by-product hydrogen is recycled through the reduction unit.

The Bosch reaction occurs at 800 to 1000 K (980 to 1340 F) in the presence of an iron catalyst with an overall result represented by:

$$CO_2 + 2\ H_2 \rightarrow C + 2\ H_2O.$$

Intermediate reactions produce CO and CH_4 which reach equilibrium concentrations established by reactor temperature, pressure, and relative proportions of the primary reactants, CO_2 and H_2. Complete conversion is obtained by recycling the process gases and continuously removing water.

A carbon dioxide reduction unit using the Bosch reaction and a continuous carbon removal approach was included in the integrated life support system (ILSS) developed by Convair and delivered to the NASA Langley Research Center under Contract NAS1-2934 (Ref. 1). After delivery of the ILSS, Convair participated in the operation, maintenance, modification, and evaluation of the integrated system and individual subsystems under Contract NAS1-5837. During this period, the Bosch reactor showed good processing characteristics when operable but required excessive mechanical maintenance and frequent repairs (Refs. 2, 3). Attempts to achieve reliability by modifying the unit were not successful. The problems originated primarily from difficulty in (1) separating carbon from the catalyst plates, (2) transporting the removed carbon to a collection point, and (3) avoiding carbon-forming reactions in regions where carbon deposits could not be tolerated.

An engineering prototype carbon dioxide reduction unit using the Bosch catalytic reaction and expendable catalyst cartridges was developed and delivered to the NASA Langley Research Center under Contract NAS1-8217 (Ref. 4). The unit had two reactors, each capable of reducing the carbon dioxide produced metabolically by a four-man crew. The dual-reactor system allowed catalyst cartridge exchange without process interruption. Cartridge life at a four-man CO_2 reduction rate was approximately three days.

Material combinations and engineering techniques developed during the experimental phase were effectively used to retain all carbon formed within the catalyst cartridge and avoid carbon-forming reactions outside the cartridge. No attempt was made to minimize power consumption or gross and expendable weights.

A "Research" reduction unit for generation, confirmation, and refinement of design concepts and for materials screening and selection tests was built and operated with independent research and development funds from 1969 through 1971 (Refs. 5, 6, 7). The initial cartridge for this single-reactor unit was intended to have a 9-man, 3-day capacity based on scaling factors developed from earlier units. However, these proved conservative since the unit was capable of operation at a 12-man level for 3 days or a 9-man level for 4 days.

At the beginning of the present contract, a dual-reactor CO_2 reduction unit using the Bosch catalytic reaction was fabricated for developing and demonstrating improvements in the areas of weight, power, volume, operability, and maintainability. This unit is called the Advanced Experimental Demonstration Unit. Many design changes were suggested during 650 hours of operation of the dual-reactor configuration. A major change was accomplished by separating the reactors into two independent units. This provided a beneficial component redundancy, simplified the changeover procedure, and improved the potential for reducing recycle compressor power. With these units, significant advances were made in compressor power conservation, process rate control concepts, and expendable weight and resupply volume reduction possibilities. A thermal modeling and computer analysis program was initiated to define and assist in resolution of difficulties experienced in meeting heat exchanger and insulation quality goals. The factors involved in integrated operation of the Bosch CO_2 reduction unit, CO_2 electrochemical depolarized concentrator (EDC), and water electrolysis unit were analyzed and experimentally simulated. The reduction unit process rate controls experienced no difficulty in responding to simulated variations in EDC performance. Details of these contract results have been reported in References 8 and 9. A comprehensive study was also made to evaluate several environmental control system (ECS) configurations using the Bosch CO_2 reduction process in comparison with several ECS configurations using the Sabatier CO_2 reduction process when each is integrated with the reaction control system (RCS) so as to use gaseous biowastes for propellants (Ref. 10) and for the case of no gaseous venting except at selected times (Ref. 9).

During the period covered by this report, the independent units were used to continue parametric studies, materials research, and power reduction efforts until fabrication of a Bosch reactor utilizing low-temperature elastomeric seals for all closures made previous reactor configurations obsolete.

2.0 DESCRIPTION OF REDUCTION UNITS

CO_2 reduction units in general consist of a high-temperature reaction section and a low-temperature control, feed, and water removal section. These sections are separated process-wise by a recuperative heat exchanger which is normally located in the high-temperature section for optimum use of insulation. The "Advanced Experimental Demonstration Unit" originally consisted of two high-temperature seal reactors with crossover tubing allowing one or both to be operated using a single compressor, condenser, and feed gas section as diagrammed in Figure 2.1 and described more fully in Reference 8.

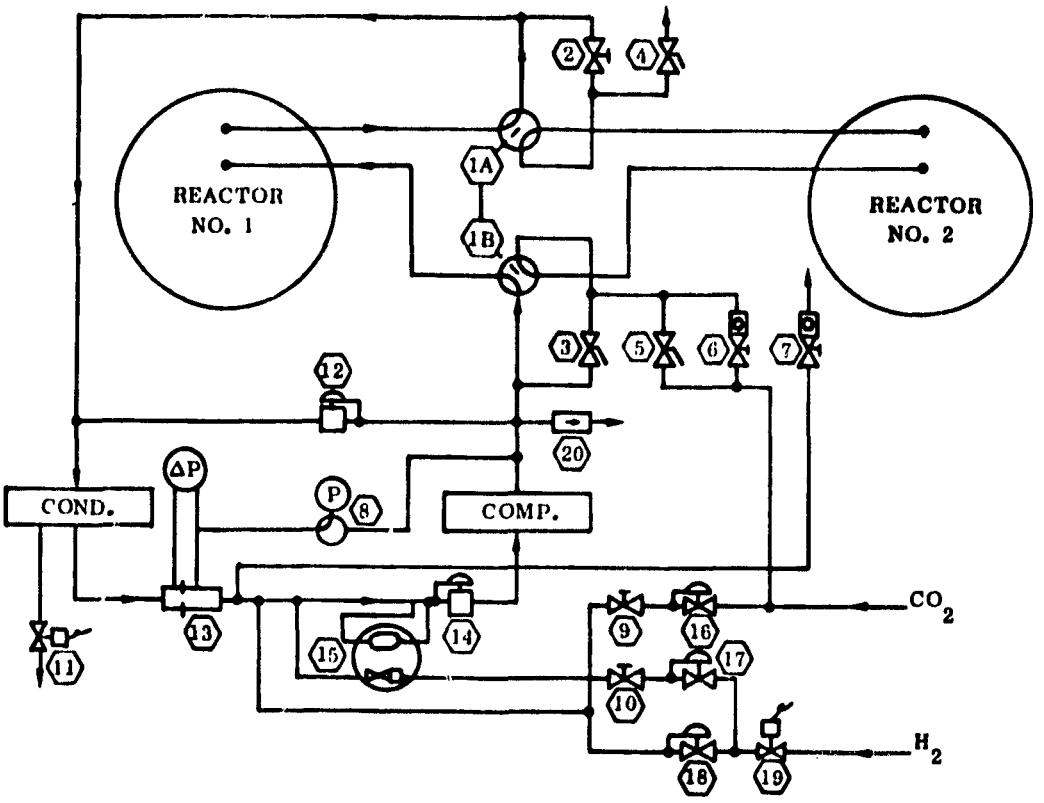

1. Reactor Selector
2. Selector Bypass Control
3. Selector Bypass
4. System Vent
5. Purge
6. Leakage Meter
7. Contaminant Bleed
8. Pressure Point Selector
9. CO_2 Feed Restrictor
10. H_2 Feed Restrictor
11. Water Removal
12. Safety Bypass
13. Recycle Flowmeter
14. Recycle Flow Control
15. Mixture Control
16. CO_2 Feed Pressure Regulator
17. H_2 Feed Pressure Regulator
18. H_2 Feed During CO_2 Failure
19. H_2 Safety During Power Failure
20. Safety Pressure Relief

Figure 2.1 - Dual Reactor CO_2 Reduction Unit Flow Diagram

This configuration was modified by separating the reactors into two independent units, each having its own compressor, condenser, and feed gas section but designed to share a feed gas source and vacuum purge system as shown in Figure 2.2.

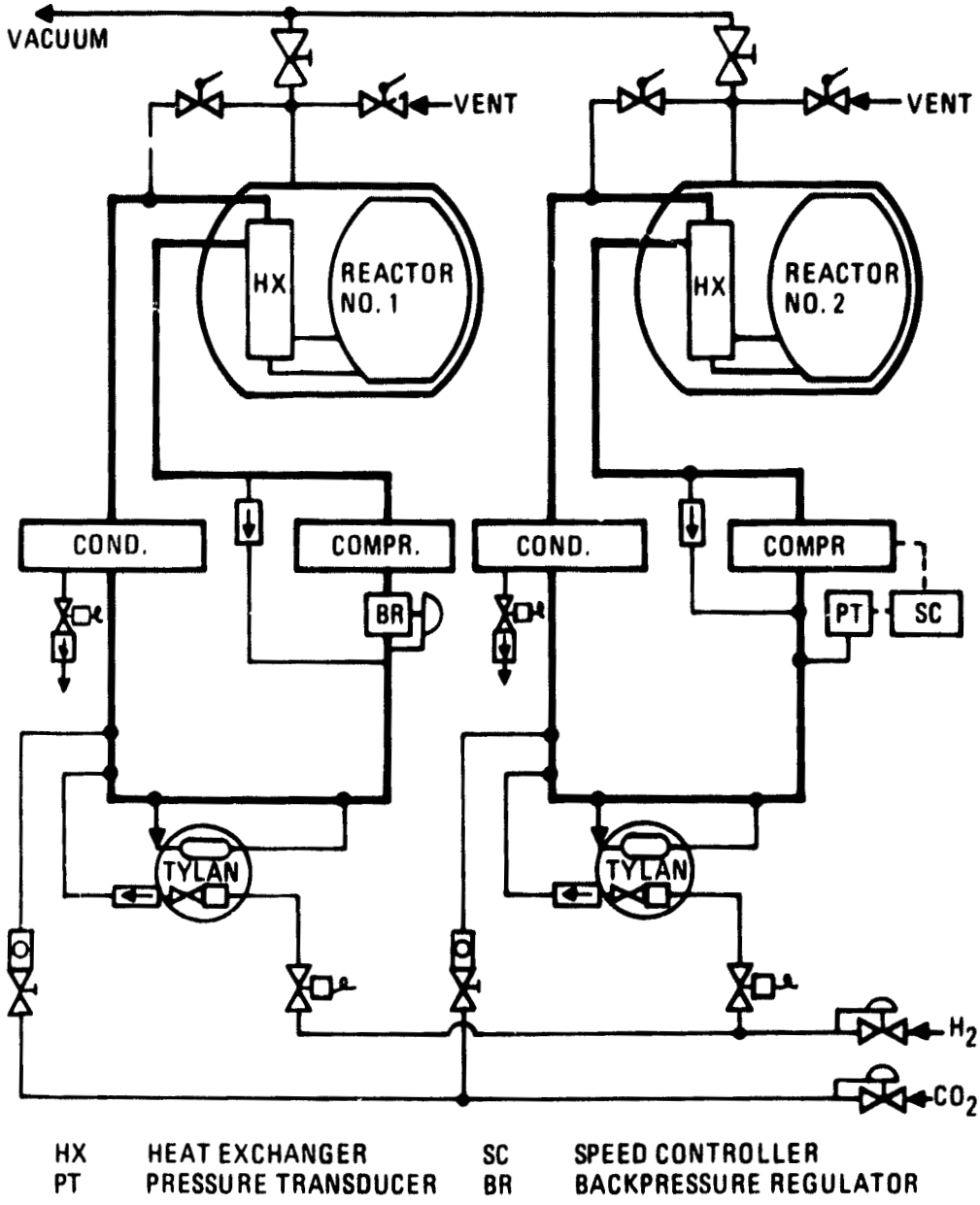

Figure 2.2 Schematic of Independent CO_2 Reduction Units

Subsequently, a reactor incorporating low-temperature seals was combined with one of the independent unit control sections as shown in Figure 2.3.

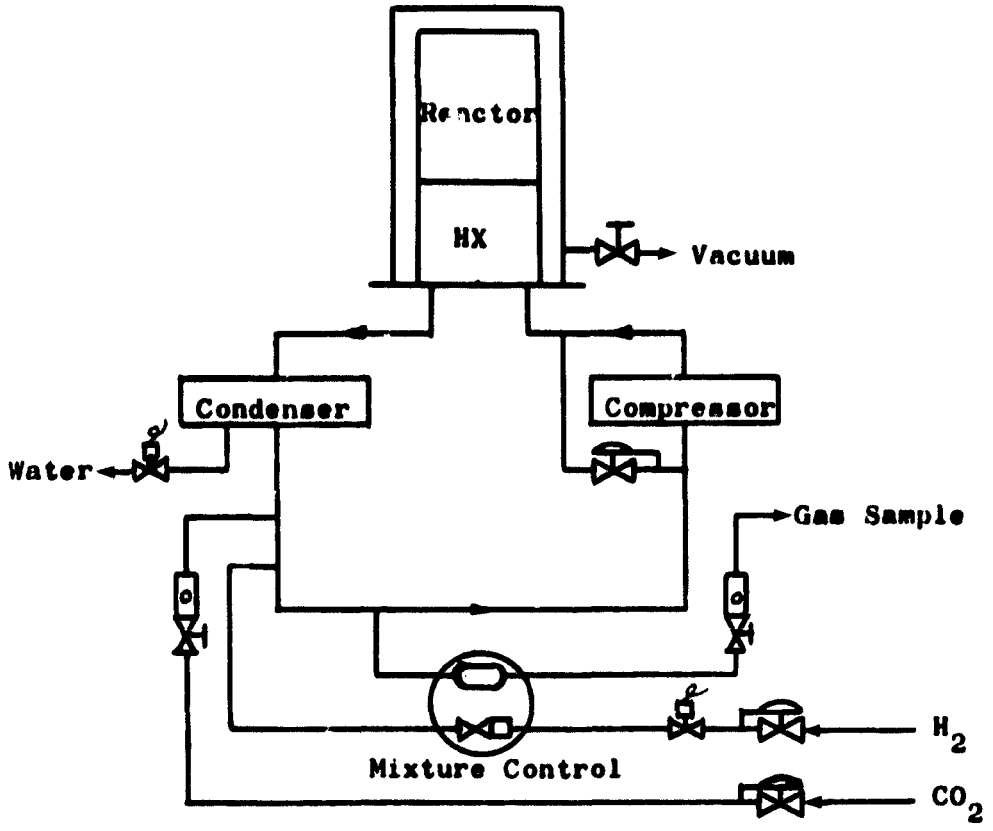

Figure 2.3 - Cold-Seal Reactor CO_2 Reduction Unit

2.1 High Temperature Section of Hot-Seal Units

Figure 2.4 is a photograph of an independent CO_2 reduction unit with the hot-seal reactor configuration and Figure 2.5 is a sectional view of the components of its high temperature section which includes the recuperative heat exchanger, reactor sub-assembly, and insulation package.

2.1.1 Recuperative Heat Exchanger. - The heat exchanger consisted of 16 formed convolutions of .254 mm (.010-inch) Inconel 625 with 5.08 mm (.20 inch) pitch, 17.8 mm (.7 inch) span, 86 mm (3.4 inch) width and 254 mm (10.0 inch) outside diameter enclosed in an annular shell as sketched in Figure 2.6.

2.1.2 Reactor Assembly. - To avoid high differential thermal expansion stresses and simplify reactor shell plating procedures, an adapter section interconnected the heat exchanger, heater shroud, heater, and reactor support shaft with the reactor shell. A studded flange was welded to the base end of the reactor to receive the adapter. The reactor shell was plated with electroless nickel. The

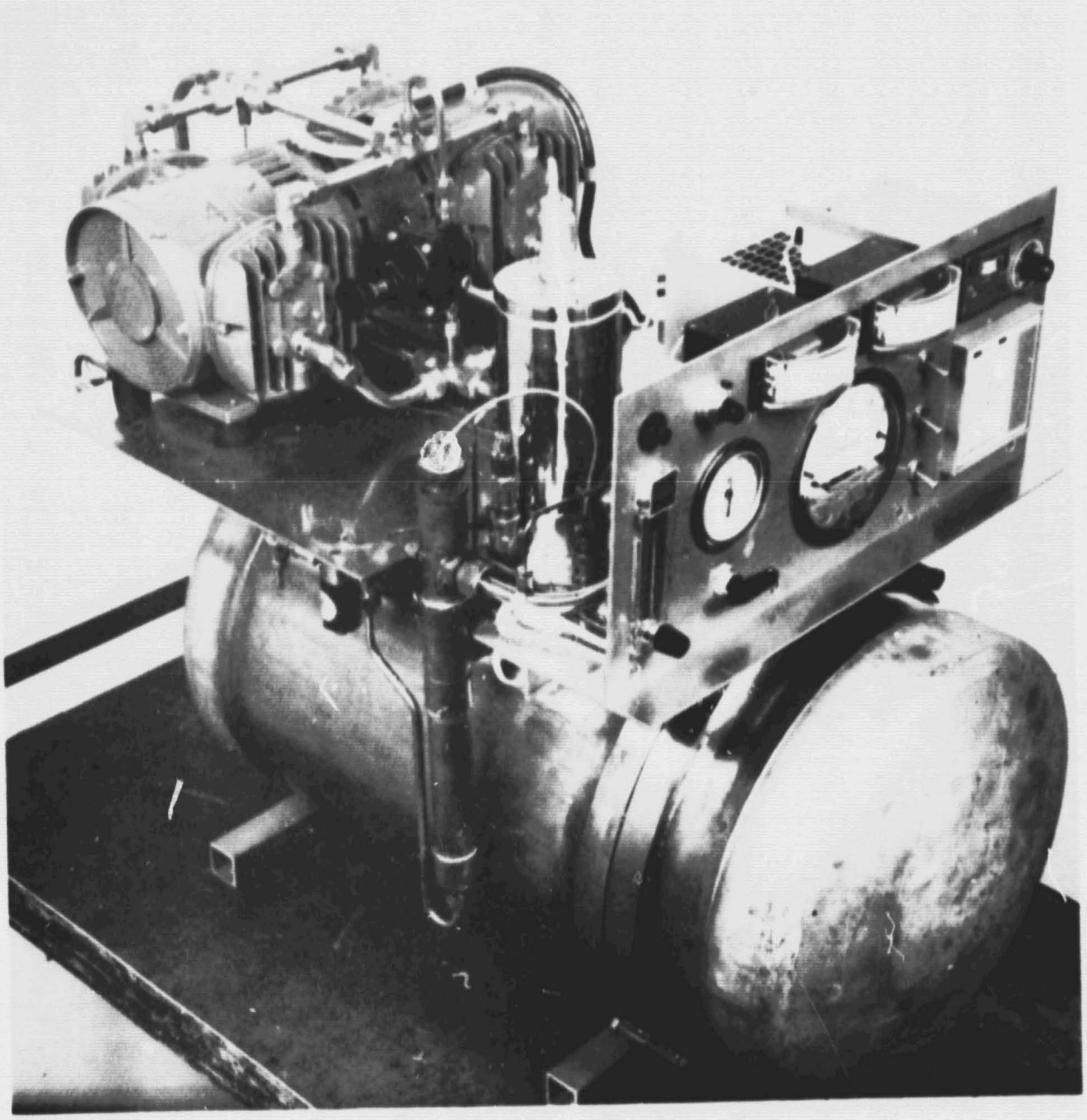

Figure 2.4 - Independent Unit General Arrangement

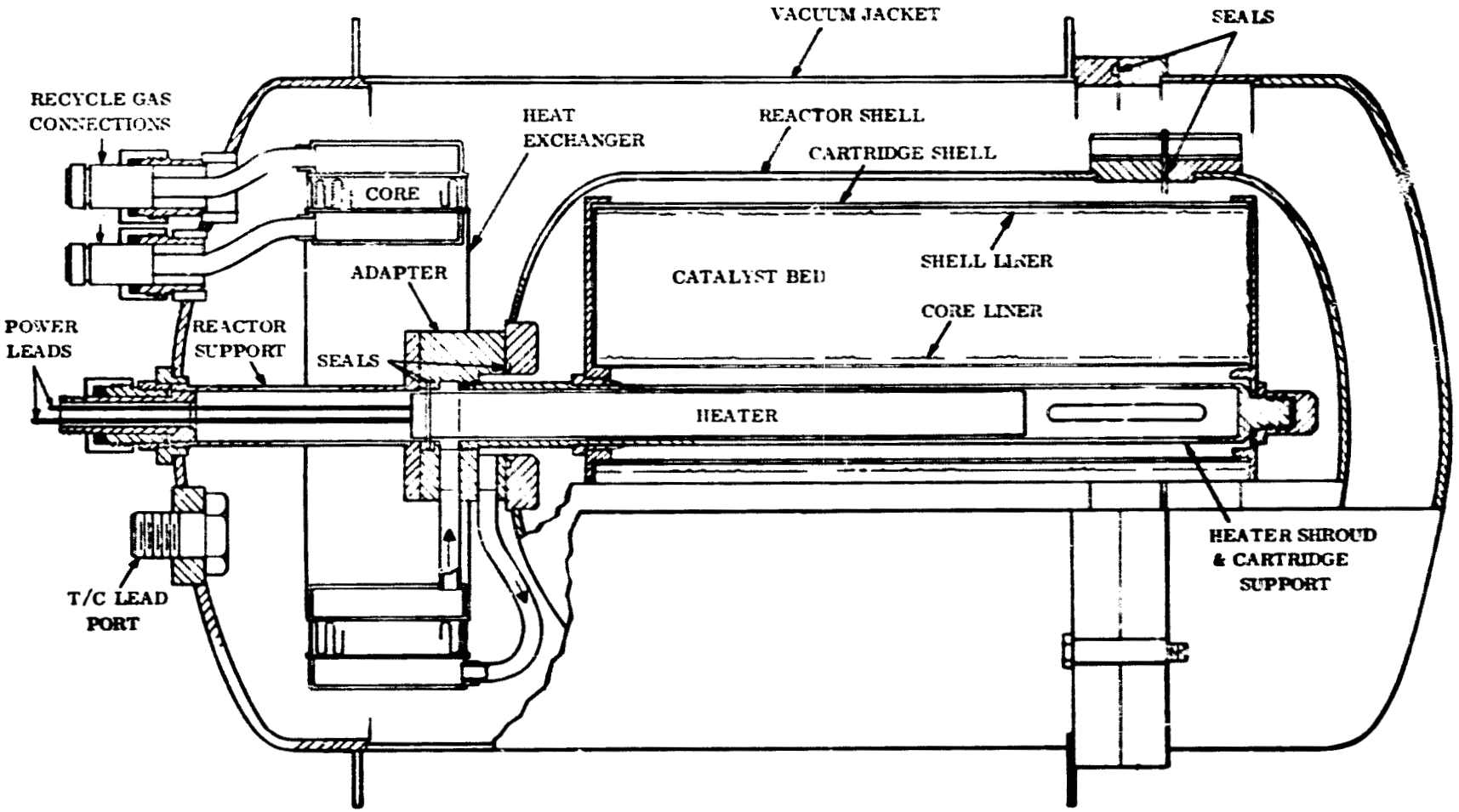

Figure 2.5 - Independent Unit High-Temperature Section

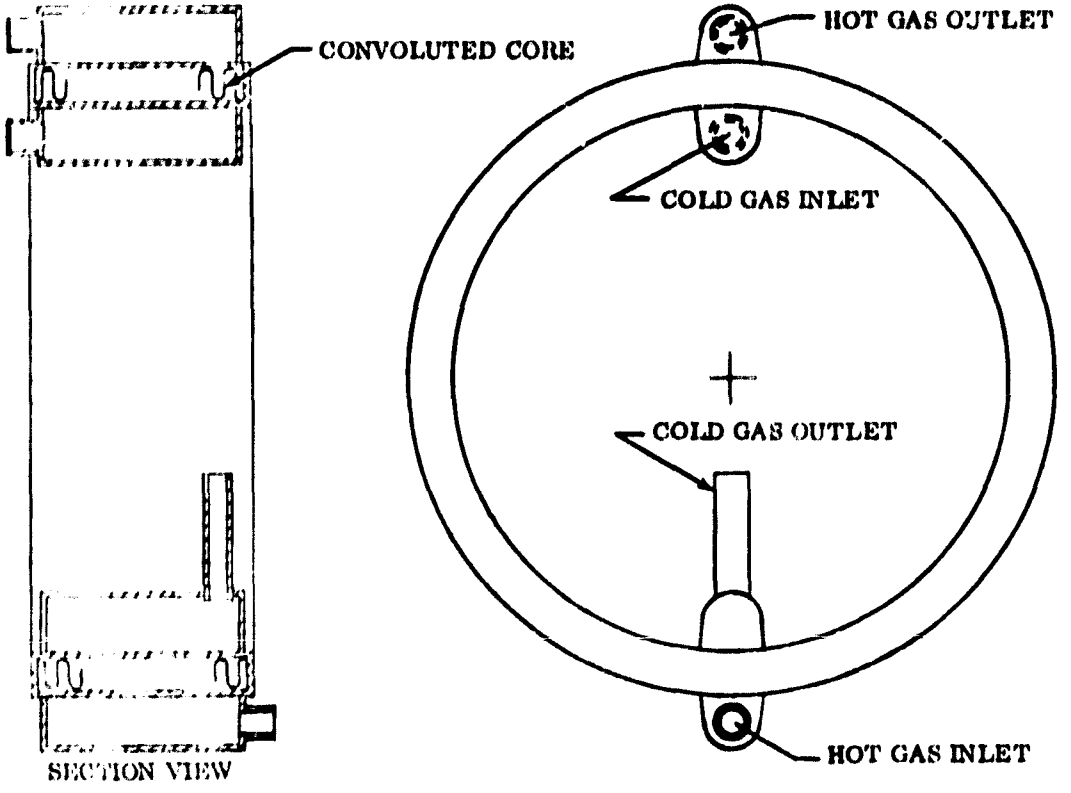

Figure 2.6 - Formed-Convolution Recuperative Heat Exchanger

adapter and shroud were made of Inconel 625 so they would not require plating and would not raise differential thermal expansion stresses where welded to the tubes from the heat exchanger. Belleville spring washers were used to take up the differential thermal expansion between the Type 304 stainless steel studs and the Inconel 625 adapter. They maintain firm loading of the aluminum bronze seal rings between the adapter, stud flange, and heater flange.

2.1.3 Thermal Insulation and Instrumentation. - The hot-seal independent units use multilayer insulation located within an evacuated zone between the reactor and vacuum jacket. Silver radiation shields of .0508 mm (2.0 mil) thickness were used in the hotter sections near the reactor shell. Aluminum shields of .0318 mm (1.25 mil) thickness were used outboard of the silver shields. The shields were separated by .952 cm (0.375 inch) Microquartz or .0798 cm (0.0313 inch) Astroquartz blankets to minimize radial conduction.

The cylindrical section had two Microquartz blankets with a silver shield between them and five silver shields separated by Astroquartz blankets. These were followed by four aluminum shields with Astroquartz separators.

The aft dome had three Microquartz blankets between the reactor and the heat exchanger with silver shields between the blankets. The center of the heat exchanger was backed with Microquartz. The insulation on the cylindrical section extended far enough to enclose the heat exchanger. From the heat exchanger to the vacuum jacket, two Microquartz blankets with a silver shield between them was used. This was followed by seven silver shields separated by Astroquartz blankets followed by an aluminum shield and two Microquartz blankets.

The end cap insulation was installed in three parts. Six silver and six aluminum shields separated by Astroquartz blankets and followed by two Microquartz blankets were placed in the end cap and held in place by a Microquartz blanket installed circumferentially in the end cap. Within this latter blanket was placed a separate insulation package consisting of six silver shields and five aluminum shields separated by Astroquartz. This third section butted against the insulation on the reactor when the end cap was installed.

Twenty thermocouples were attached to the reactor shell, adapter, heat exchanger and insulation jacket shell to determine the performance of the insulation and heat exchanger. An additional thermocouple was attached to the reactor shell to provide a signal for the temperature controller.

2.2 High Temperature Section of the Cold-Seal Unit

The fundamental concept of the cold-seal reactor is that shells, supports, instrumentation leads, and power lines originating in the hot region and requiring gas tight seals are extended to a distance sufficiently removed that heat losses due to longitudinal conduction are acceptably low and temperatures at the sealing point are within the working range of elastomeric materials. This tends to increase the overall length but has several significant advantages over hot-seal configurations.

The arrangement of the components in the high temperature section of the cold-seal unit is shown in Figure 2.7. These components include the recuperative heat exchanger, catalytic reactor, thermal insulation and temperature instrumentation.

2.2.1 Cold-Seal Recuperative Heat Exchanger. - The recuperative heat exchanger of the present cold-seal reactor uses three concentric (Inconel 718) shells to provide heat transfer surface area and counterflow passages for the process gas entering and leaving the reaction zone. These shells are supported by flanges at the

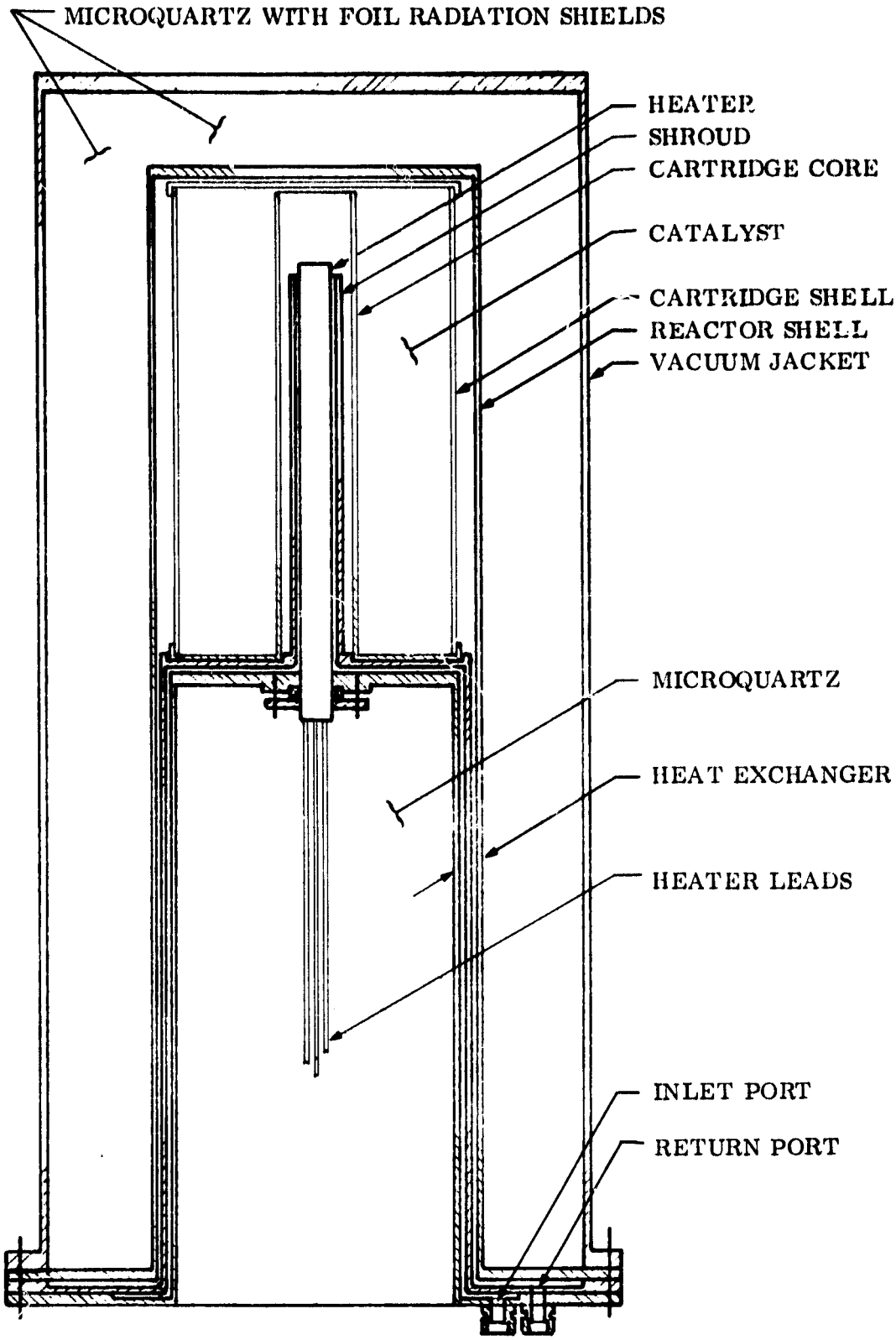

Figure 2.7 - Cold-Seal Reactor Assembly

cold end which are machined to provide distribution manifolds for the inlet and outlet ports and grooved for elastomeric seals to prevent external leakage. The head of the inner shell supports an electric heater and also forms one wall of the passage directing flow to the annulus between the heater and heater shroud. The middle shell provides the heat transfer surface between incoming and return gases and its head serves as the opposite wall of the passage directing flow to the heater. The outer shell is continued to also serve as the reactor wall.

2.2.2 Cold-Seal Reactor Assembly. - The catalytic reactor boundaries are formed by the extended portion and head of the outer heat exchanger shell and the middle shell head. This region contains the recycle gas heater, heater shroud and catalyst cartridge. An aluminum bronze seal between the heater flange and its support plate represents the only deviation from the cold-seal philosophy. Flexible loading of this seal is maintained by Bellville spring washers.

The reactor was sized to process the CO_2 from four men for a five-day cartridge exchange cycle after an initial evaluation indicated the cost of a scale model would not be significantly less. The cartridge consists of a perforated core welded to a base plate, perforated outer shell, cover plate, ceramic fiber liners, and steel wool catalyst. The metal components were of Type 304 stainless steel with an aluminide coating to prevent catalytic activity. Core and shell diameters were 44.5 mm (1.75 inch) O.D. and 221 mm (8.70 inch) O.D., respectively, and the shell length was 356 mm (14 inches).

2.2.3 Thermal Insulation and Instrumentation. - Insulation was required around the reactor/heat exchanger shell and within the inner shell to provide protection and conserve heat. The upper 254 mm (10 inches) of the inner shell were fully packed with Microquartz followed by a 102 I.D. by 229 O.D. by 229 mm (4 I.D. by 9 O.D. by 9-inch) long muff of Microquartz which allowed access to heater power and thermocouple lead connections. This region contained no thermal radiation shields and was exposed to ambient pressure.

The reactor/heat exchanger shell was insulated by 12 layers of Microquartz, each surrounded by a foil radiation shield. The upper 508 mm (20 inches) of the three shields closest to the reactor section were of 0.0508 mm (2.0 mil) silver to withstand the high temperatures involved. The rest of the shields were of 0.0318 mm (1.25 mil) aluminum. The shields around the heat exchanger section were interrupted frequently to minimize longitudinal conduction to the assembly base. The top of the reactor was insulated with 14 layers of Microquartz with 7 silver and 7 aluminum shields. This insulation package was enclosed in an aluminum jacket bolted and sealed to the reactor flange so the assembly could be removed for cartridge exchange. A counterweight and pulley system assisted in handling the assembly. A port was provided in the aluminum shell allowing a vacuum to be maintained for improved insulation performance.

To obtain thermodynamic information, 20 thermocouples were attached to the heat exchanger, reactor, and vacuum jacket shells and the inlet and outlet gas ports. An additional thermocouple was attached at the midpoint of the reactor shell and connected to the reactor temperature controller. The leads from the thermocouples within the vacuum jacket were attached to the pins of a hermetically sealed bulkhead fitting through the top of the jacket.

2.3 Low Temperature Section

Low temperature sections generally include a compressor, water vapor condenser, process rate controls, and monitoring equipment. Since the low temperature section of one of the independent hot seal units was eventually incorporated in the cold seal unit without significant alteration, the following descriptions apply to both assemblies.

2.3.1 Compressor. - A compressor is required to recycle the process gases through the reactor as product water vapor is removed by the condenser. A Thomas Industries Model 4907 QA-18 four cylinder diaphragm type compressor with integral one-third horsepower, three-phase, 208 volt, 60 Hz motor was used. The three-phase motor allowed speed control by power input from a variable-frequency supply.

2.3.2 Water Removal Components. - Gas returning from the reactor through the recuperative heat exchanger is further cooled to condense the product water vapor and allow the reduction process to continue. If this is not done, an equilibrium is soon reached and further reaction ceases. Gravity-independent operation was not required for this program so a commercial concentric tube type of heat exchanger with fins on the gas side was modified to improve the coolant-to-inner-tube heat transfer rate and to provide a water collection reservoir. High and low water level sensing probes were installed in the reservoir to operate a solenoid valve for automatic water removal. A manually operated switch also allowed the water level to be drained to the low level without being triggered by the high level probe.

2.3.3 Controls and Instrumentation. - Control capabilities are provided for start-up and shutdown; for operational flexibility and experimentation; and for unattended operation during most of each cartridge life cycle. Sufficient instrumentation is installed to provide data necessary for successful operation and for evaluating the various measures of performance. The process rate is primarily influenced by recycle flow rate, gas mixture composition, and reactor temperature. The most immediate response can be gained by altering the flow rate. Therefore, the composition and temperature controls are used primarily to maintain set-point values.

Two solid state temperature controllers with adjustable set points are required for each reactor. One senses and limits heater sheath temperature to avoid burnout and the other controls heater power to maintain a selected reactor shell

temperature. They incorporate proportional, rate, and reset action to provide set-point control without "overshoot".

The recycle gas composition is monitored and controlled by an instrument which detects the thermal conductivity of the recycle gas and positions a modulating hydrogen feed valve to maintain a set point thermal conductivity of the mixture. A hydrogen feed flowmeter is also integral with this unit. Both the hydrogen flow and the recycle gas thermal conductivity are displayed on meters on the front panel. Samples of recycle gas obtained through the contaminant bleed valve and flowmeter assembly are analyzed with a gas chromatograph for actual gas compositions. The feed gases, CO_2 and H_2, enter the unit through pressure regulators. A feed restrictor valve and flowmeter assembly between the CO_2 regulator and recycle loop performs process rate adjustment and monitoring functions.

Components of the low temperature section are arranged to accept three process rate control modes involving automatic recycle flow adjustment. One method automatically modulates the recycle flow to a constant-speed compressor by means of an in-line back pressure regulator set to maintain the desired feed-point pressure. In the closed system under normal feed supply conditions, a reduction in process rate due to adverse changes in temperature, pressure differential, mixture, etc., will tend to increase the total system pressure, including that at the feed point. Within the capacity limits of the back pressure regulator and compressor, this tendency is resisted by opening of the regulator to increase the recycle flow and, thereby, the process rate. If the process rate is too high, the feed-point pressure tends to fall causing the regulator to restrict recycle flow. This method has the advantages of operational simplicity and low initial cost but the throttling process represents an inherent non-productive consumption of power.

A second method maintains a constant feed-point pressure by means of a sensitive pressure transducer that signals the compressor motor to change speed as required to maintain the match between process and feed rates. This method has definite power-saving possibilities but is somewhat more expensive, more complex, and due to the added complexity, perhaps less reliable.

The third technique retains the simplicity, reliability, and low cost of the first method without in-line throttling losses. A delivery pressure regulator by-passes recycle flow from the constant speed compressor back to the feed section as required to maintain a constant feed section pressure. This results in lower pressure ratios and consequently lower power consumption until full capacity of the compressor is required.

Compressor outlet and feed section pressures are measured with a single gage by using a two-position selector valve, thereby reducing errors in determining the pressure differential.

A portion of the recycle loop is instrumented and calibrated for flow versus pressure drop allowing recycle gas flow rate data to be obtained without dissipating additional compressor energy.

3.0 TECHNICAL DISCUSSION

Operational data for approximately the first half of this period of the contract was obtained from the independent hot-seal reduction unit described in Section 2. Extensive information concerning configuration influence, materials performance, and catalyst response to contaminants was obtained during 680 hours of operation of this unit but problems with heat exchangers, seals, and material reactions made a data base for parametric analyses and power studies difficult to establish. The cold-seal unit subsequently provided a significantly improved device for isolating parametric and contaminant effects and for power reduction observations. The most important features of this unit are the reliability of its seals and the ease with which the reactor/heat exchanger section can be completely disassembled revealing all surfaces exposed to reactive conditions. During 2335 hours of cold-seal unit operation, the observations and data taken were specifically addressed to process rate control modes, heat exchanger performance, heat losses of the high temperature assembly, electric power consumption of the compressor and heater, catalyst packing, hardware configuration evaluations, and materials studies.

3.1 Process Rate Control Mode Selection

As discussed in Section 2.3.3, the backpressure regulator and compressor bypass regulator modes of process rate control are both effective and uncomplicated but the backpressure regulator mode is not competitive energy-wise because it acts as an inline throttle. Energy requirements of the compressor bypass regulator and variable speed modes are quite similar and each mode has advantages in different mission situations. Figure 3.1 shows the results of a comparison test of the two modes. To eliminate the effects of dissimilar catalyst packs, temperatures, process rates, mixtures, etc., the data were obtained concurrently from a single run by stabilizing conditions with one mode, then switching to and adjusting the alternate mode to maintain the same process rate. With the bypass closed, the lowest speed control setting produced a 5-man process level during periods when conditions were optimum so this level was maintained for the duration of the run. Compressor speed for the bypass mode was held at 83.8 radians per second (800 revolutions per minute) since this speed was required to maintain the process level at the end of the run. If an earlier cutoff point had been chosen, for example when the pressure differential reached 27.6 kN/m^2 (4 psi), a lower speed setting could have been used and the comparison curves would have been correspondingly closer together.

The speed control power curve does not include the power required for conditioning a pressure transducer signal to the controller nor the controller input power. Assuming a 90 percent efficiency for a controller designed to the required load range and adding 5 watts for signal conditioning, the comparable curves expressed on a per man basis are plotted in Figure 3.2.

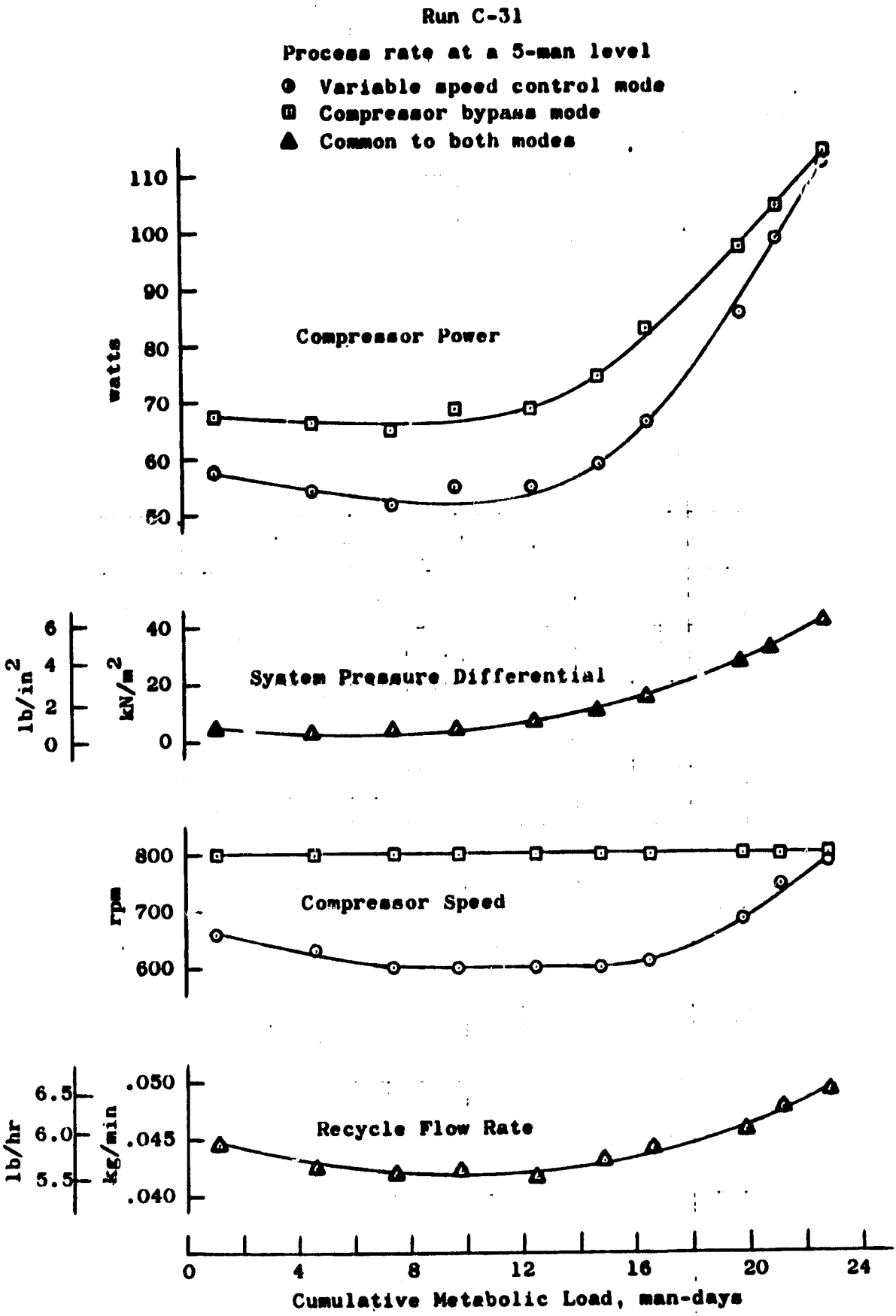

Figure 3.1 - Control Mode Data

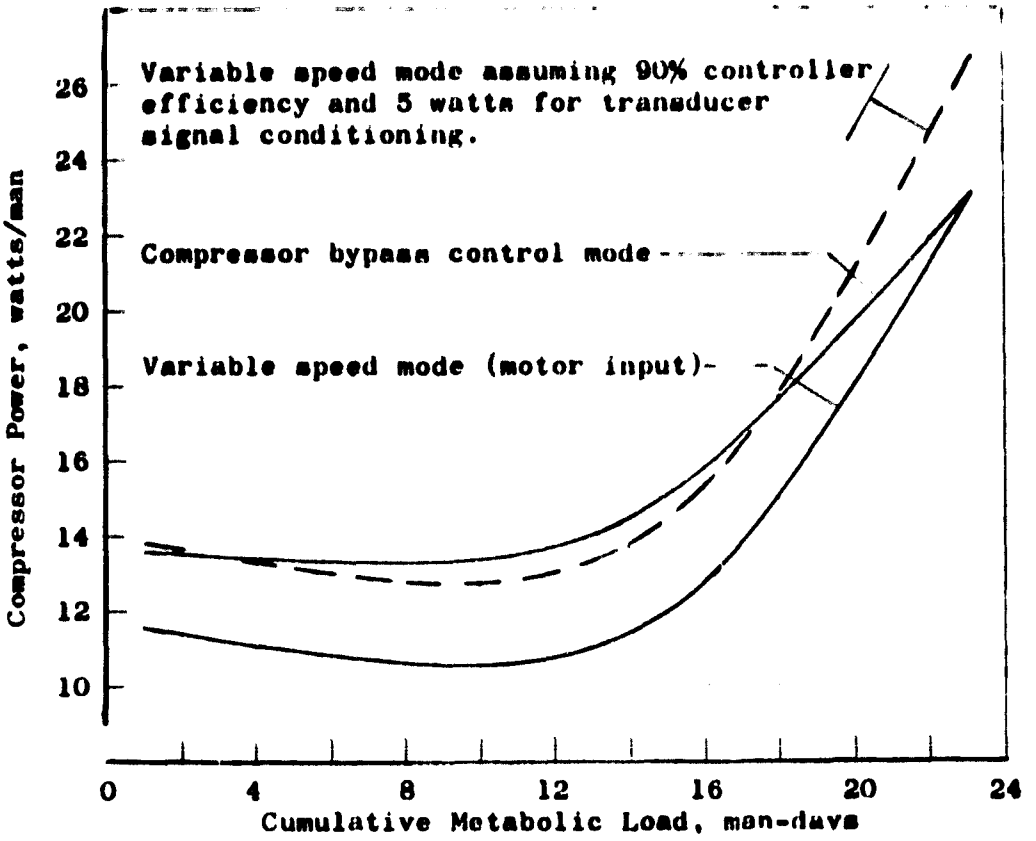

Figure 3.2 - Control Mode Power Comparison

For a constant process rate requirement, it is apparent that the added complexity of the speed control mode is not justified. However, a mission for which the rate requirement varied appreciably, for example from a 4-man level to a 6 or 8-man level and return, the compressor would have to be sized for the highest rate and the bypass mode would waste more power at the 4-man level than would the speed control mode. A possible compromise would be to use a manually switched two-speed motor with the compressor bypass pressure regulator.

3.2 Heat Exchanger Performance

Observed performance was compared with predicted performance over a range of recycle gas compositions and flow rates. The range of parameters was consistent with measurements taken during the last ten runs of the unit, which provided a total of more than 1000 operating hours. Start up transients were excluded. Heat exchanger performance was expressed in the conventional manner as an effectiveness, ϵ_T, where the measured value is:

$$\epsilon_T = \frac{T_{Hot_{in}} - T_{Hot_{out}}}{T_{Hot_{in}} - T_{Cold_{in}}} .$$

The measurements were made with chromel-alumel thermocouples on the heat exchanger surfaces. Predicted performance was calculated from heat transfer parameters and included a correction for longitudinal conduction in the metal.

3.2.1 Gas Composition Effects. - Recycle dry gas compositions were measured by gas chromatograph and adjusted to the nearest increments of 5 mol percent. There were 25 such compositions observed, the five most frequent being 45/20/20/15, 50/25/10/15, 45/25/15/15, 50/20/15/15, and 40/25/20/15 mol percent respectively of $H_2/CO/CH_4/CO_2$. The average of 143 data points was 45/20/20/15, which was also the most frequent observation.

Calculations showed heat exchanger effectiveness to be only slightly sensitive to gas composition within the usual ranges. Mixtures of the same H_2 content, with normal variations in CO, CH_4, and CO_2, have almost identical calculated performance. Figure 3.3 shows results for the H_2 range from 40 to 50 mol percent.

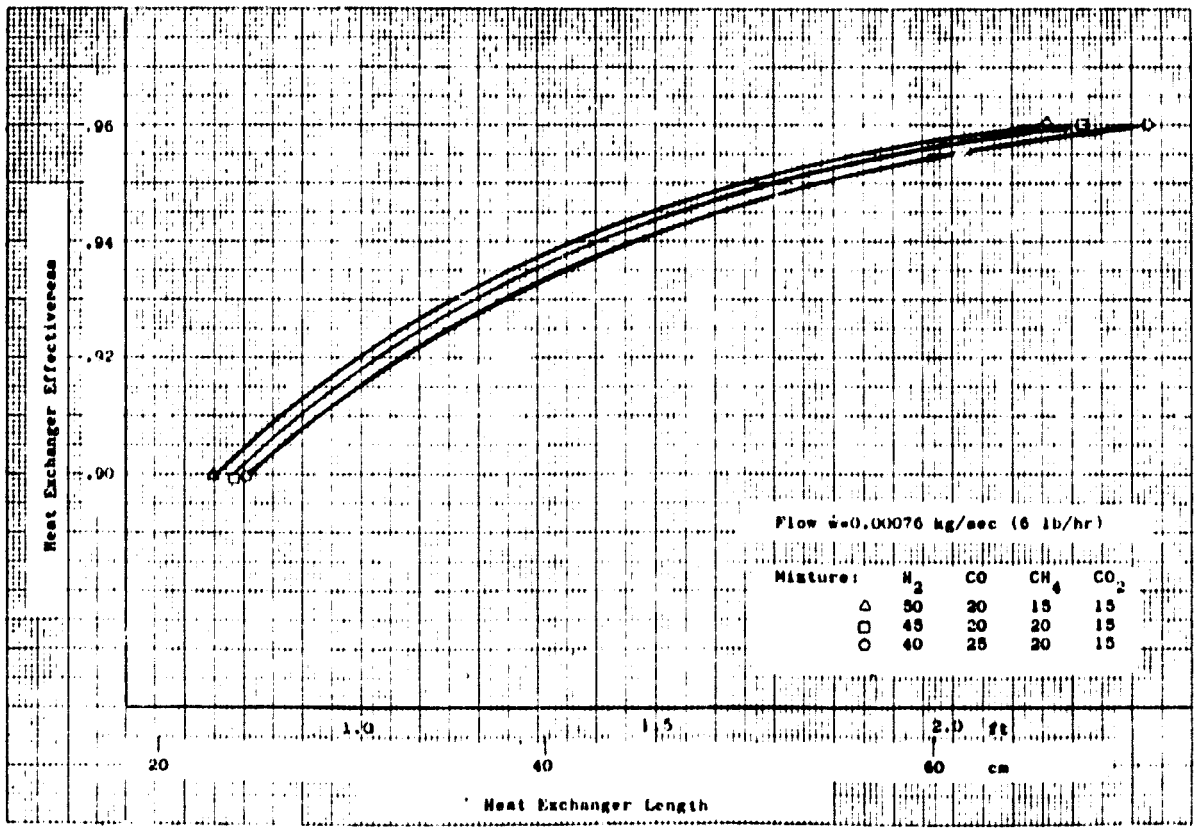

Figure 3.3 - Calculated Effects of Gas Composition on Heat Exchanger Performance

3.2.2 Gas Flow Rate Effects. - Calculations for the five most frequent gas compositions showed effectiveness also to be only slightly sensitive to recycle flow rate within the normal range of 0.0005 to 0.001 kg/sec (4 to 8 lb/hr). Figure 3.4, for a mol percent composition of 50 H_2/25 CO/10 CH_4/15 CO_2, is typical of these results. Slight differences for other compositions were consistent with the trends previously shown in Figure 3.3. Calculated effectiveness versus flow for the design point length of 45.7 cm (1.5 feet) is also shown in Figures 3.5 and 3.6. These curves are the predicted performance.

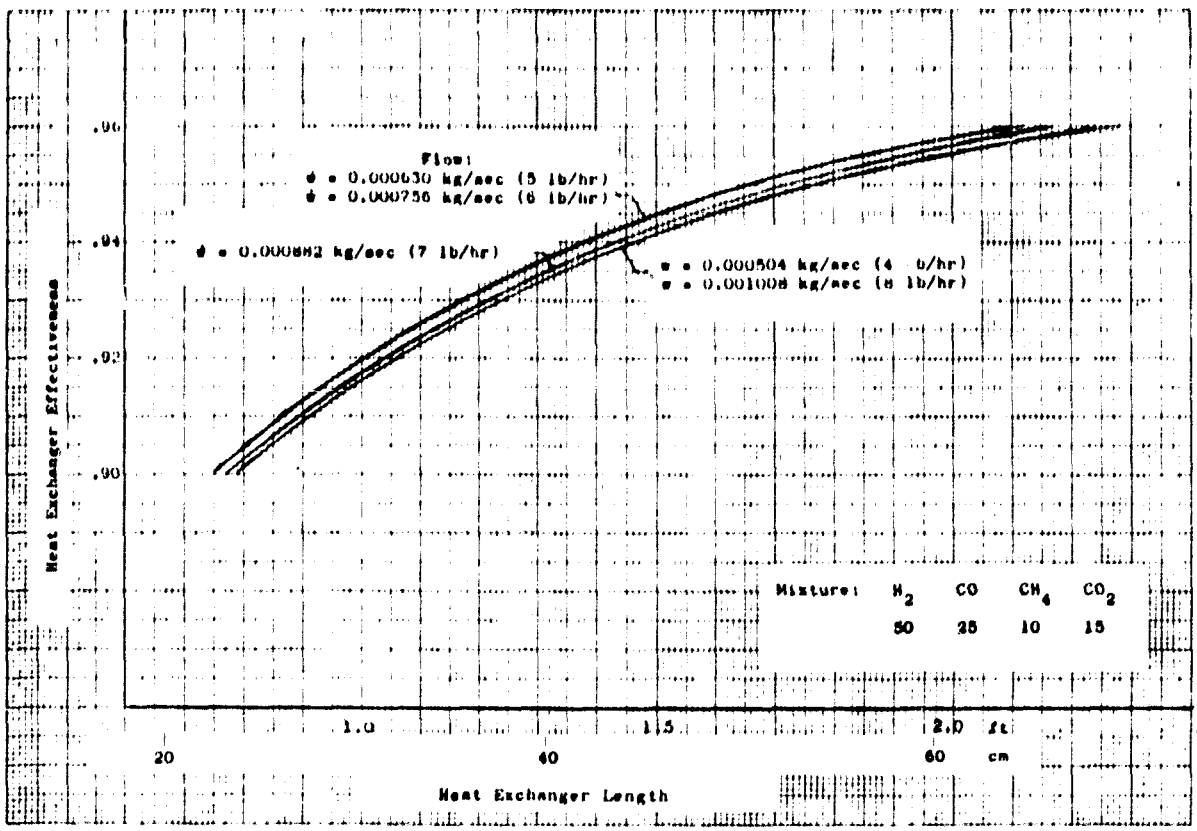

Figure 3.4 - Calculated Effects of Gas Flow Rate on Heat Exchanger Performance

3.2.3 Measured Performance. - Temperature data points were selected from several runs to determine the "measured performance". This selection took all points of the average mol percent composition of 45 H_2/20 CO/ 20 CH_4/15 CO_2, and these points were plotted in Figure 3.5. A least squares data fit to an assumed straight line characteristic was calculated for comparison with predicted performance, and shows agreement within one percent effectiveness value.

The excessive scatter of the points in Figure 3.5 reflects temperature data scatter, which prompted an instrumentation change. The analog type temperature

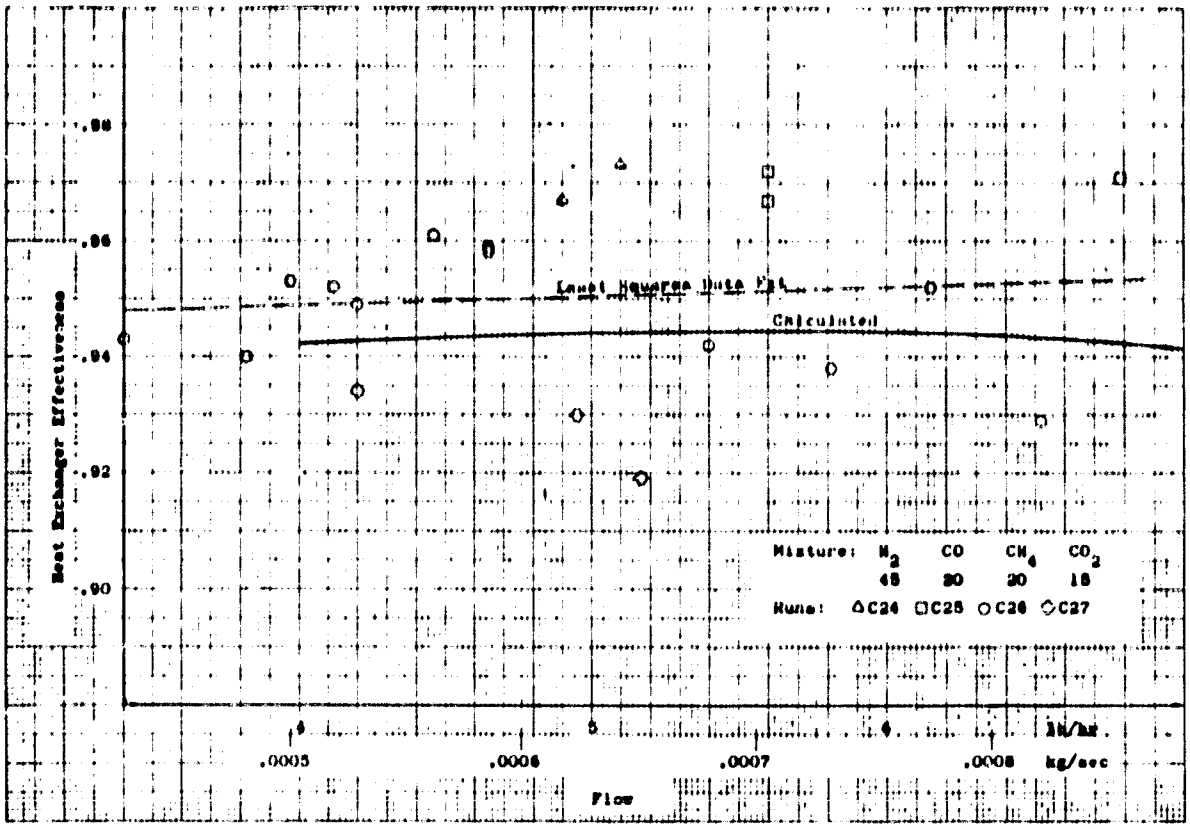

Figure 3.5 - Heat Exchanger Predicted and Measured Performance, 45% H_2

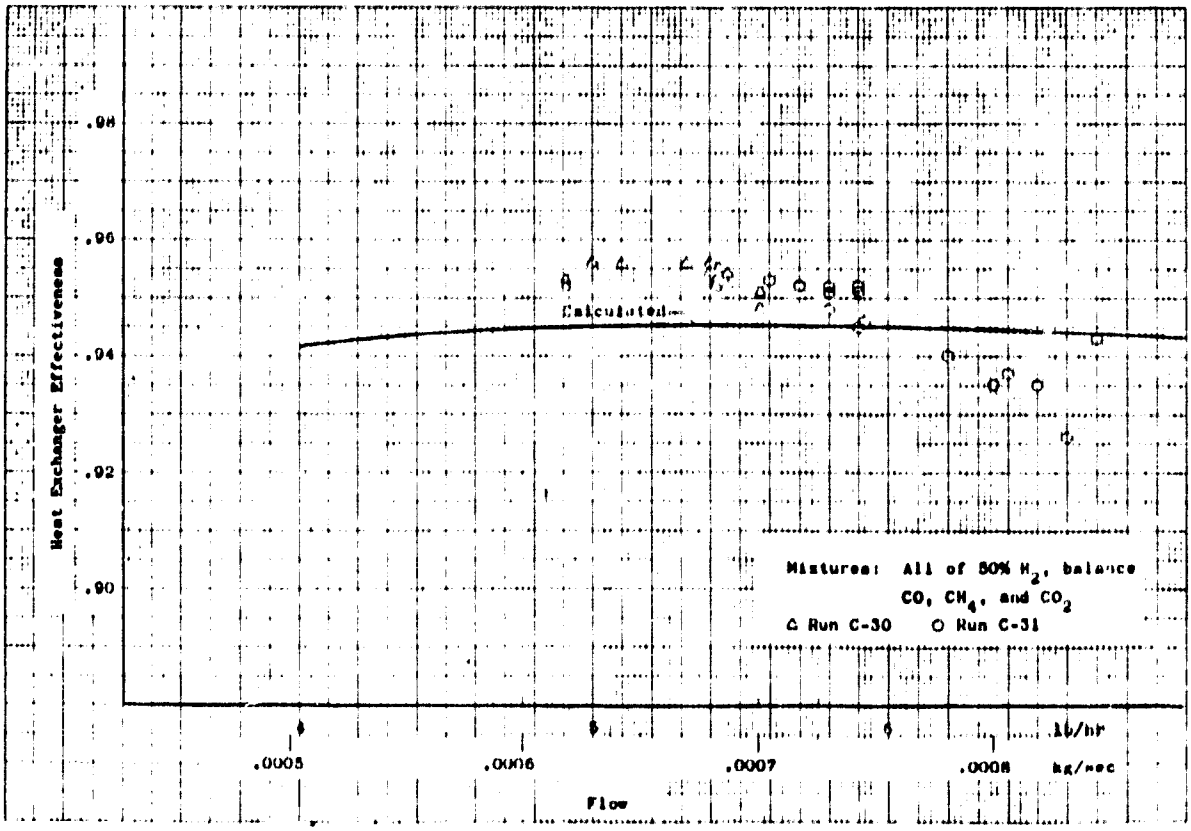

Figure 3.6 - Heat Exchanger Predicted and Measured Performance, 50% H_2

readout meter was replaced with a digital type. Data of the two subsequent runs was used for Figure 3.6. In this case, the most frequent composition was at 50 mol percent H_2. Since the influence of variations in percentage of the other gases had been shown to be negligible, all data points of 50 mol percent H_2 were used. There is much less scatter, which confirmed the instrumentation change, and there is fairly good agreement with predicted performance.

3.2.4 Heat Exchanger Performance Conclusions. For purposes of heat exchanger performance evaluation, the influences of mixture and flow rate variations were so small that average values could have been used without invalidating results. There were much greater uncertainties in the accuracy of temperature measurements and in the question of whether the measured values reflected real gas temperatures. The good agreement between measured and predicted performance in Figure 3-6 suggests that both the analytical methods and the instrumentation techniques were reasonably satisfactory.

Exclusion of data points associated with start up transients has been mentioned. There is probably also reason to exclude data points at and near the end of a run, although this was not done. Transients were evident, and appeared to cause the greater discrepancies between measured and predicted performance.

3.3 Reactor Assembly Heat Losses

Heat energy enters the reactor/heat exchanger assembly by recycle gas transport, exothermic heat of reaction, and electrical resistance heater input. It leaves by recycle gas transport, and by convection and radiation from the vacuum jacket and base. Heat reaches the jacket and base by conduction through the insulation and cartridge support structure which, in the cold seal unit, consists of the heat exchanger shells. The net gas transport heat flow is primarily a function of the performance of the recuperative heat exchanger. During stabilized operation, the heater makes up the deficiency by which heat losses exceed heat gains. Power penalties make it worthwhile to reduce this deficiency to a practical minimum. It is theoretically possible to operate solely on the heat of reaction but the required improvement in insulation may not be practical to obtain.

Computer models of the hot and cold-seal units were set up to obtain detailed patterns of temperature distribution and heat transfer throughout the unit. The objective was to develop a basic procedure whereby configuration concepts could be rapidly evaluated for future design guidance. An existing thermal analyzer computer program, compatible with the CDC Cyber 70 Scope 3.4 system and capable of handling problems approaching 2000 nodes and 4000 resistors with unlimited node-resistor arrangements, was tried. Heat exchanger design calculations were supported but overall heat balances were not obtainable without extensive program modifications

to properly model the distribution of recycle flow through the reaction zone and recombination for return through the heat exchanger.

Power loss distributions for the cold-seal unit have been calculated from observed data. Thermocouples were used to measure recycle gas temperatures entering and leaving the assembly. The flow rate was determined from the pressure drop through a calibrated section of the recycle loop with corrections applied for variations in temperature, pressure, and gas characteristics.

Chromatographic analysis of recycle gas samples established the composition for which the gas constant, specific heat, and viscosity were determined. The net heat loss by recycle gas transport was then calculated using the equation,

$$q_t = \dot{w} (T_{out} - T_{in}) C_{p_{av}}$$

where,

q_t = gas transport heat loss

$C_{p_{av}}$ = mean specific heat

$\dot{w}$ = recycle flow rate

T = gas temperature.

The combined heat transmission through the support structure and insulation package is dissipated by free convection and radiation from the various surfaces of the enclosing shell. These were calculated using the equations,

$$q_c = h_c A (T_s - T_a)$$

and

$$q_r = \epsilon \sigma A (T_s^4 - T_a^4)$$

where

q_c = convective heat loss

q_r = radiative heat loss

h_c = film conduction coefficient

ϵ = surface emissivity

σ = Stefan-Boltzmann constant

A = surface area

T_s = surface temperature

T_a = ambient temperature

Suitable emissivity values were selected for the surface conditions and film conduction values for the various surface orientations were calculated using procedures suggested in Reference 11. Calculations based on support cross-section area, length, thermal conductivity, and temperature differential were used to separate the support heat flow from the total surface heat dissipation to determine the loss chargeable to insulation.

A wattmeter was used to monitor heat input power and the heat of reaction was calculated on the basis of 27.5 watts per man-level of operation.

Reactor assembly power distribution and heat balance data for Run C-31 are plotted in Figures 3.7 and 3.8. These curves show that major gains are not likely to be made in reducing gas transport heat losses which are already quite low because of good heat exchanger performance. Support structure heat losses, although quite low, could be trimmed a few watts by increasing the path length and reducing the transfer area. The general insulation, which allows about 75 percent of the accounted-for losses, could be improved by using better quality radiation shielding and more meticulous assembly techniques. These improvements could probably reduce insulation losses by no more than 25 percent.

3.4 Power Consumption

The conditions that result in minimum power for one component of the CO_2 reduction unit may cause excessive power consumption in other areas. For example, operating at the lowest possible temperature may minimize insulation losses but a high recycle flow rate will be needed to maintain the required process level. This adversely affects compressor power and heat loss to the condenser. The power-influencing factors that can be manipulated during a run are the recycle gas composition, reactor temperature, recycle flow rate, and condenser temperature. The effects of catalyst preparation and packing techniques can only be determined by comparing a series of runs for which the catalyst treatment or support technique is varied. Much of the data presented in following paragraphs was taken during a period when a different catalyst support configuration was being experimentally evaluated in each successive run. This accounts for some of the run to run data scatter which tends to obscure the influence of any other parameter.

3.4.1 Electrical Power Measurements. - Heater and compressor electrical power inputs were measured separately by conventional wattmeters, and eight recent runs were selected for showing representative performance data. The measured inputs were normalized to a per man basis and averaged for each run. Data points prior to one man-day of operation and after 20 man-days were excluded so that start up and termination transients would not bias the major trends. The averages thus determined are shown in Table 3.1, from which the runs of lowest and nearest average power were

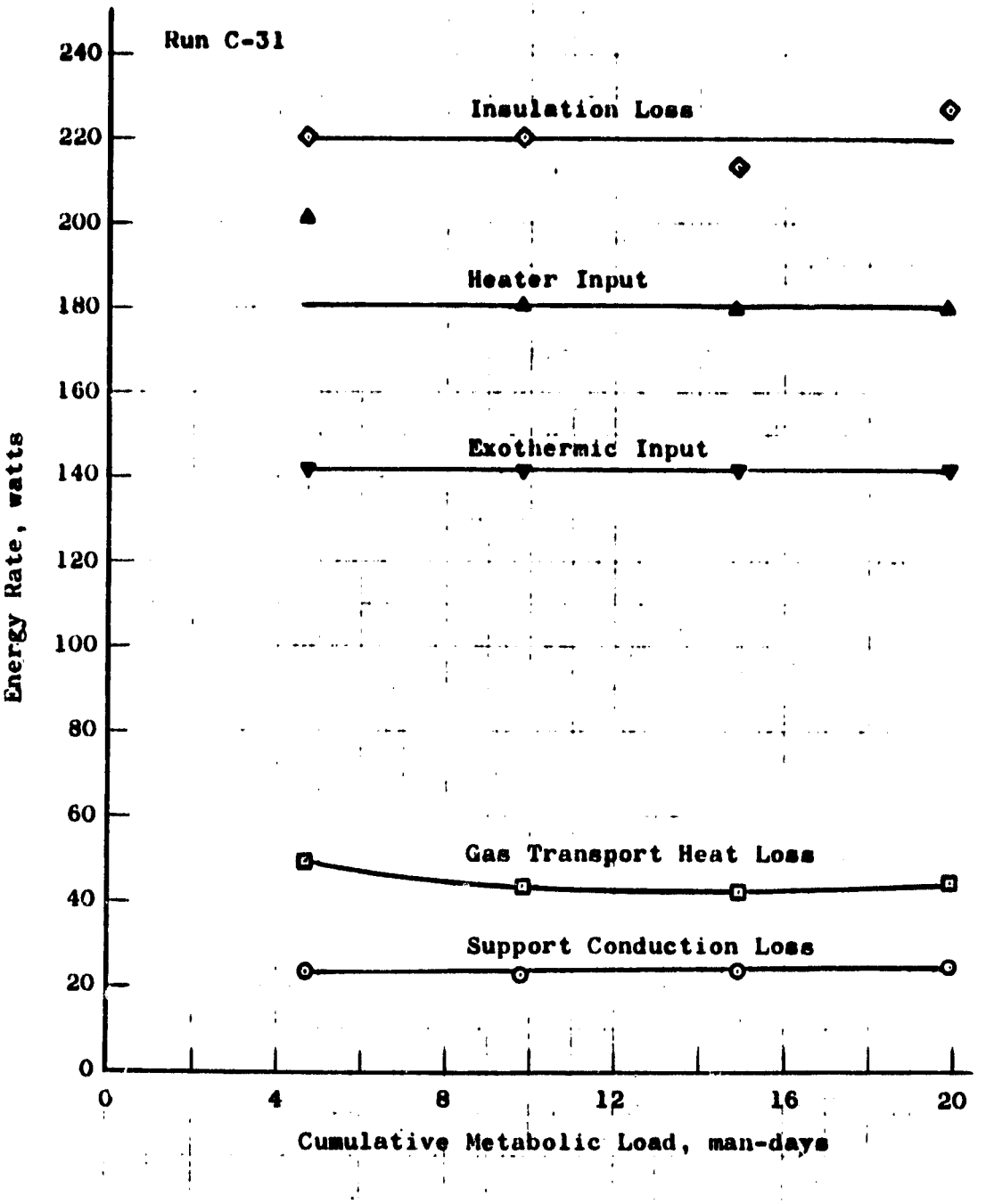

Figure 3.7 - Reactor Assembly Power Distribution

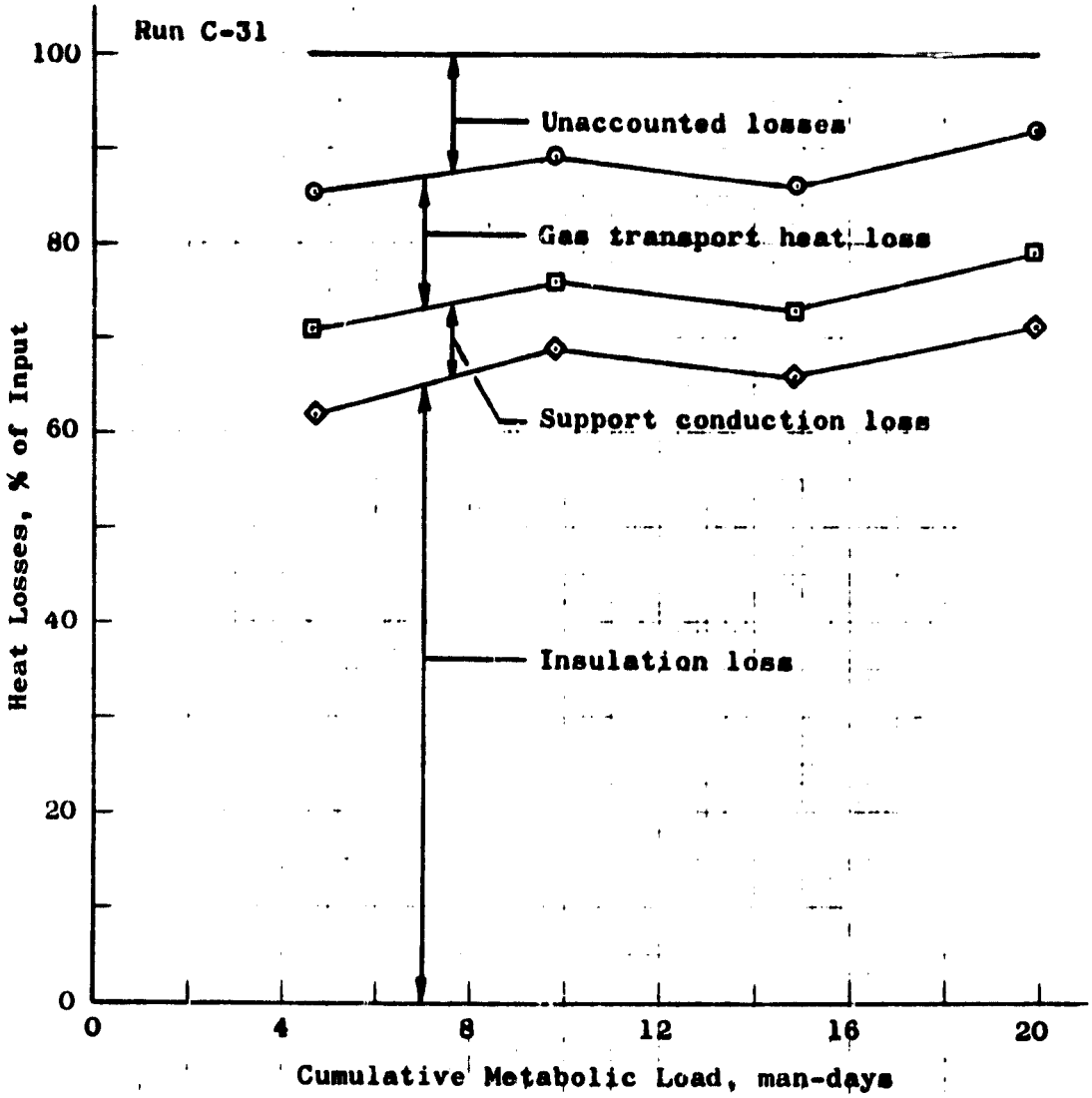

Figure 3.8 - Reactor Assembly Heat Balance

TABLE 3.1 - AVERAGE POWER INPUTS FOR EIGHT RUNS

Run No.	No. of Data Points	Average Power, watts/man			Average Flow/man		Representative H_2, mol %
		Heater	Compressor	Total	kg/sec	lb/hr	
C-21	14	40.24	16.59	56.83	0.00740	0.98	45-50
C-22	14	33.51	16.46	49.97	0.00809	1.07	40-50
C-23	14	36.25	18.79	55.05	0.00953	1.26	30-50
C-24	12	30.58	16.74	47.32	0.00816	1.08	45-50
C-25	14	37.01	16.69	53.70	0.00907	1.20	45
C-26	12	42.11	17.30	59.41	0.00900	1.19	40-45
C-30	14	34.91	16.34	51.25	0.00839	1.11	45-50
C-31	12	37.73	14.62	52.35	0.00877	1.16	50
Average	--	36.54	16.69	53.23	0.00854	1.13	--

identified. These runs are plotted individually in Figure 3.9 on a time axis normalized to cumulative metabolic load in man-days. Data for these runs was then examined for those differences in temperatures, mixtures, or other factors which would explain lower or higher than average power.

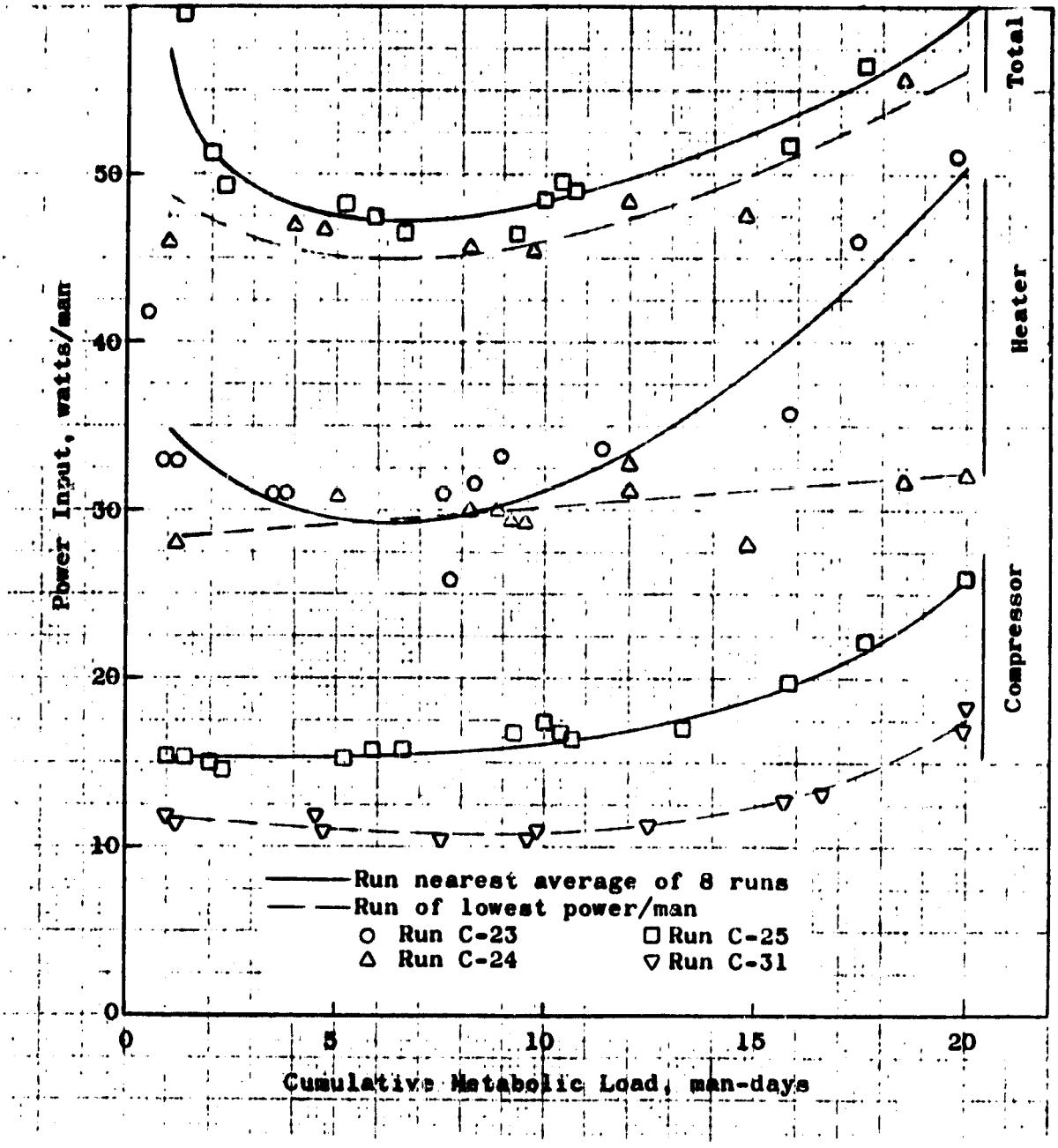

Figure 3.9 - Power Input vs. Operating Time

3.4.2 Compressor Power Performance Evaluation. - Lowest compressor power was concurrent with highest H_2 content of the gas mixture, as shown by average values in Table 3.1 and by individual data points in Figure 3.10. This is an

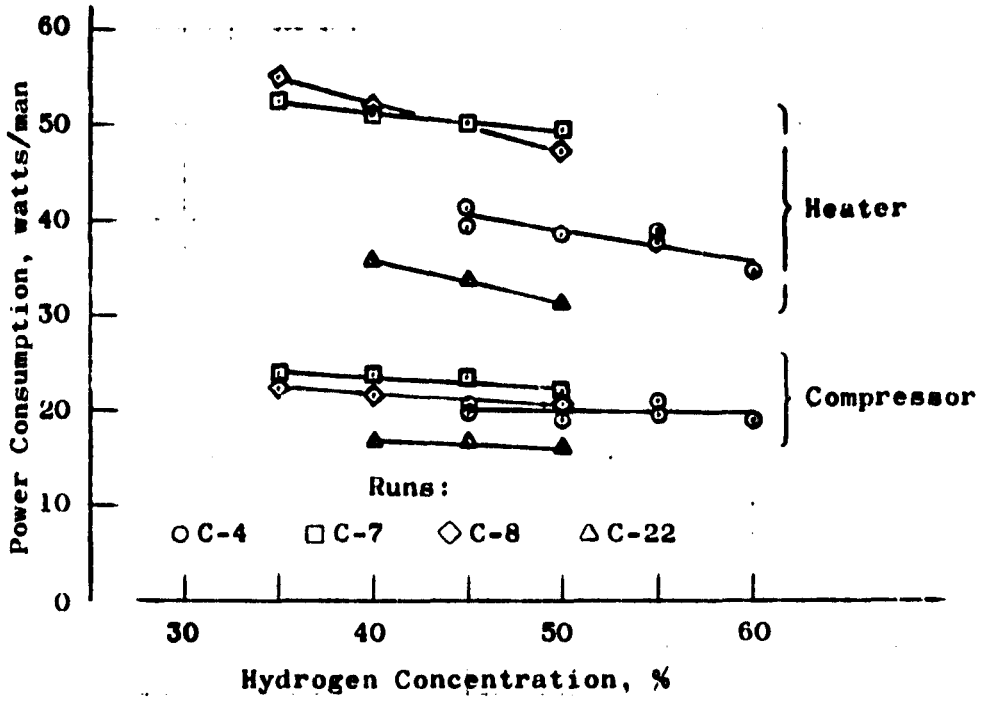

Figure 3.10 - Gas Composition Effect on Power Consumption

expected trend because mixture density and mass flow decrease with increased H_2. Reactor temperatures are not a factor except to the extent that they influence mixture composition. Compressor inlet temperature is primarily a consequence of condenser performance, and varies in a relatively small range.

3.4.3 Heater Power Performance Evaluation. - Controllable factors expected to influence heater power consumption include reactor temperature, recycle flow rate, and mixture composition. Relationships can be derived fromthe data; but they should be viewed as valid trends rather than precise correlations, due to the many variables and limited data quantity. For example, the relatively high heater power shown in Table 3.1 for Run C-21 is associated with a higher than average insulation jacket pressure (poor vacuum) and higher than average surface temperatures.

The influence of mixture composition, in particular the H_2 content, is shown in Figure 3.10. This trend toward decreasing heater power with increasing H_2 content is consistent with the mixture composition effects on heat exchanger effectiveness that were discussed in Paragraph 3.2.1 and shown in Figure 3.3. The beneficial effects of H_2 are due to its favorable heat transport properties in comparison with other gases of the mixture.

The influence of reactor temperatures on heater power is available in Figure 3.11, where total power is plotted against control temperature at separate intervals in cartridge life. Since compressor power is relatively insensitive to reactor

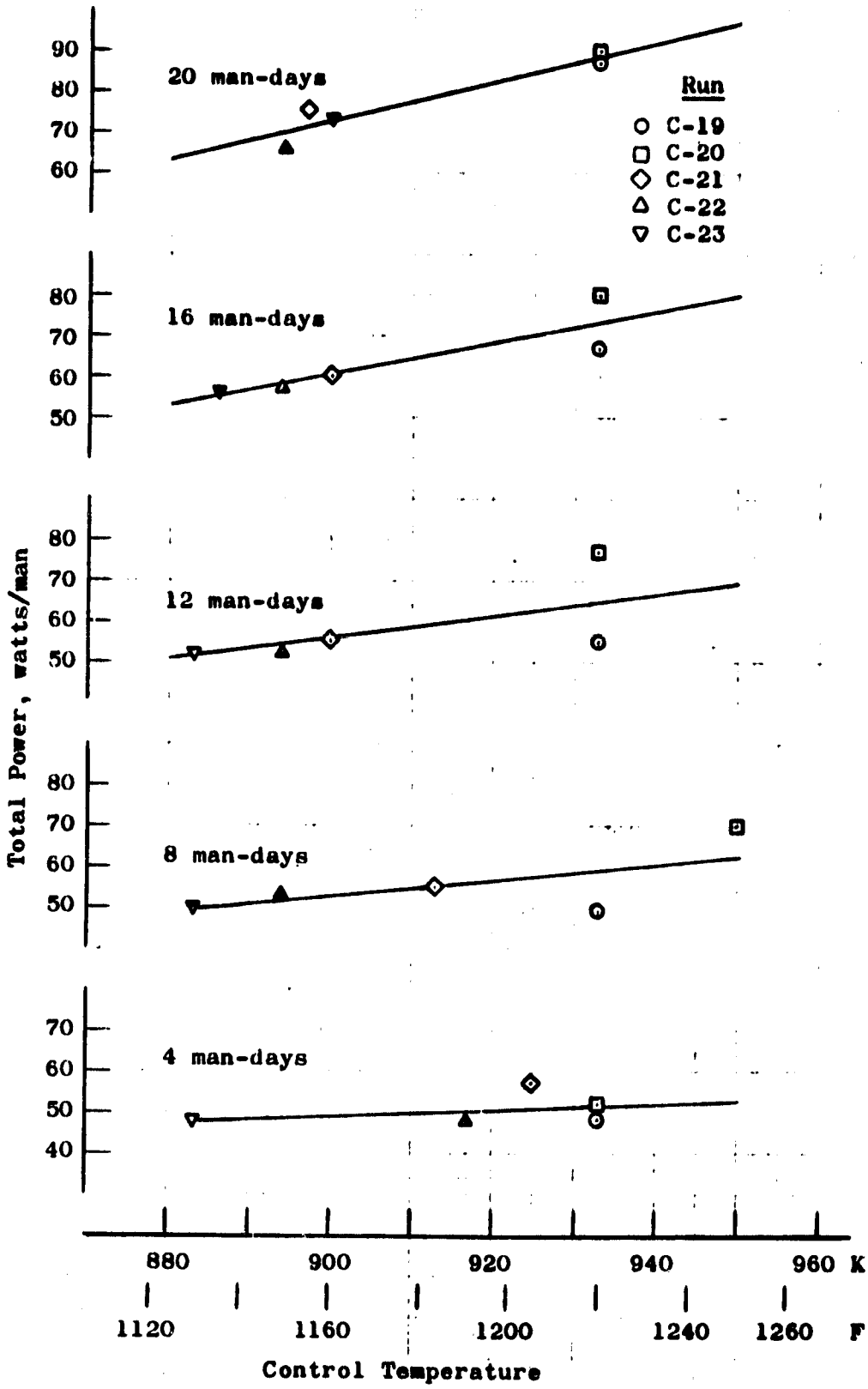

Figure 3.11 - Power Consumption vs. Reactor Temperature

temperatures, the effects shown are almost entirely due to heater power characteristics. These characteristics are also shown in Figure 3.12 where data of six runs are plotted with lines of constant recycle flow rate. Both figures show the same trend; namely, that heater power is reduced as reactor temperature is reduced. This is expected because the insulation and structural heat losses decrease with decreased temperature.

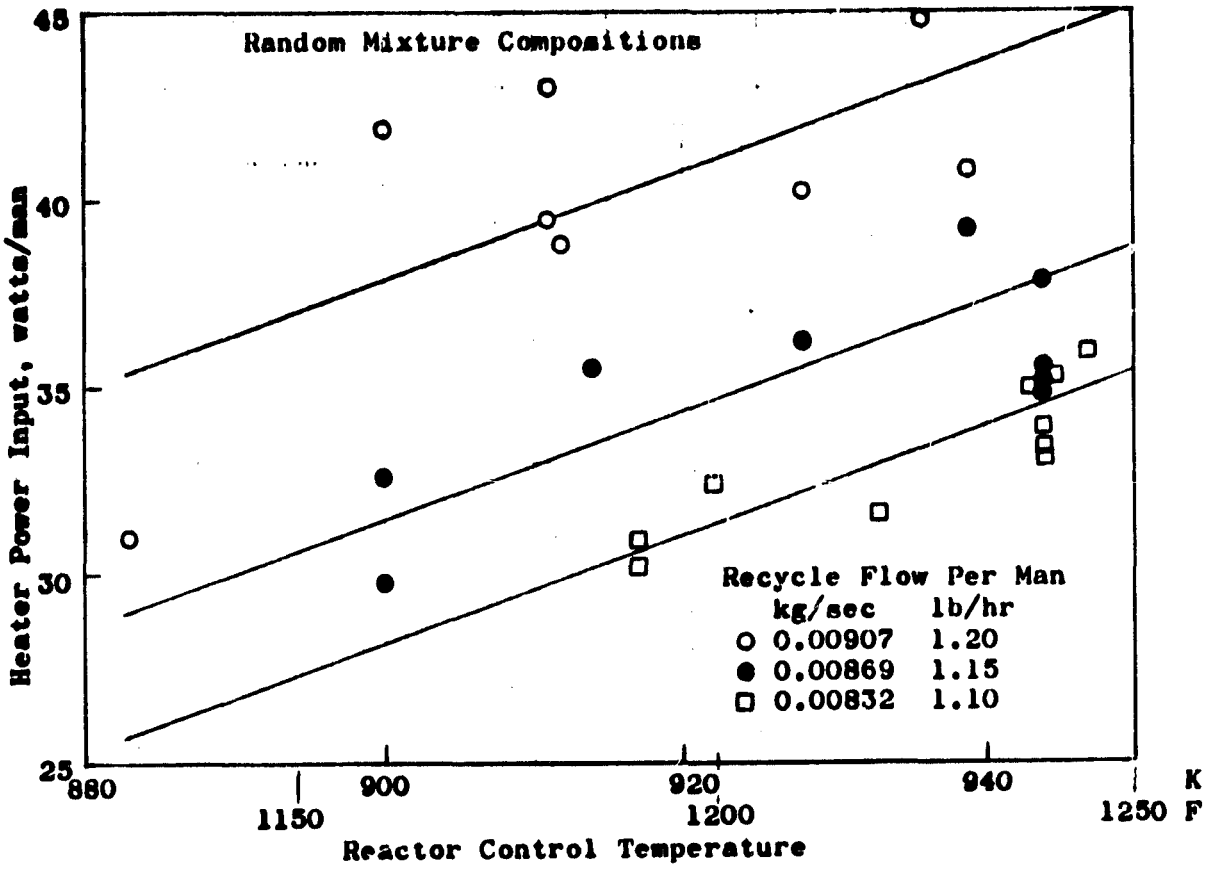

Figure 3.12 - Temperature and Flow Rate Effects on Heater Power

Figure 3.12 also shows that heater power increases with increased recycle flow rate, which is expected. Although the plotted points are at random mixture compositions and random intervals of cartridge life, the trend is clearly direct although nonlinear. The non-linearity is probably due to a nonlinear relationship of heat exchanger effectiveness with flow.

3.4.4 Power Consumption Summary. - The total power data of Table 3.1 and Figures 3.9, 3.10 and 3.11 reflects variations that were intentionally introduced to elicit effects of operating parameters and catalyst support configurations. It was shown that, within certain limits, power per man decreases somewhat with increased H_2 content and decreased reactor temperature; but much larger benefits are attained

with the best known catalyst packing and support techniques. The present state-of-the-art is represented by the best of the foregoing data, since the techniques are known and can be easily duplicated.

There is undoubtedly an upper limit for H_2 content and a lower limit for reactor temperature, beyond which reaction rate decreases would require increased recycle flow and higher power. It was not possible to determine these limits with the present mixture controller because it becomes unstable at some prior point and shuts down reactant feed. This occurs because high H_2 concentration and low temperature result in a high CH_4 content, which the controller misinterprets as excess CO_2. Since the slopes of curves in Figures 3.10, 3.11, and 3.12 are not very high, the power at optimum temperature and mixture would probably be only a little lower than the best shown in Figure 3.9.

An improvement of a few watts/man can also be expected with an optimized compressor motor.

3.5 Configuration Evaluations

Many configuration considerations affect the maintainability, operational simplicity, and performance of CO_2 reduction systems. To avoid process interruption during cartridge exchange procedures, the gas supply system can either serve two independent reduction units or a dual reactor unit that shares a single recycle compressor, condenser, and process rate controls. The internal passages of the recuperative heat exchanger can be made accessible for periodic inspection and maintenance or a more compact permanently welded construction can be used. The reactor can be designed with component and access seals exposed to the high-temperature reactive environment or remote from such exposure. Cartridge exchange procedures and catalyst support requirements are influenced by reactor orientation when gravity or acceleration forces are applied. Finally, the distribution of the catalyst within the cartridge shell can materially affect both cartridge life and the total energy expended during a mission.

3.5.1 Independent vs. Dual Units. - Earlier designs incorporated the dual reactor concept allowing the reactors to share a recycle compressor, condenser, water removal system, and process rate controls. Although this halved some component requirements, the added system complexity caused procedural problems and increased energy consumption. During start-up of the alternate reactor with a fresh cartridge, the compressor was required to supply recycle flow simultaneously to both reactors. The oversized motor and compressor unit needed during this relatively brief period could not be matched for maximum efficiency during the long periods of single-reactor operation. Additional energy was wasted in pressure losses generated by the more complicated plumbing and valving required to select

the individual reactor or allow simultaneous operation. Failure of one of the shared components of the dual unit would stop CO_2 reduction until repairs were completed, whereas with independent units the alternate one would be available to carry the load. The cool-down, cartridge replacement, and restart can be accomplished in 10 or 12 hours if necessary so one unit could handle 90 percent of the metabolic load indefinitely if the other unit was permanently disabled and no CO_2 accumulator was available. With a 12-hour accumulator capacity, a second unit might not be required but the redundancy of units as well as unit components improves system reliability.

3.5.2 Cold-Seal vs. Hot-Seal Concepts. - As previously stated, hot-seal units are so constructed that the seal for the closure allowing access for cartridge replacement and recycle gas connections between the heat exchanger and reactor are exposed to the high-temperature reactive environment. Cold-seal reactor shells, heat exchanger connections, and supports originating in the hot region are extended to reduce longitudinal conduction to acceptable values and to allow the use of elastomeric seals.

The hot-seal unit is basically more compact, requires less clearance for access to the cartridge, and has a lighter weight closure to be manipulated during cartridge exchange procedures. With the covers removed, the cartridge is not as easily manipulated as for the cold-seal unit. Reactor, heat exchanger, and insulation maintenance or repair is more likely to be required and much more difficult to perform. Closure fastening devices must have a very low profile to avoid heat shorts through the insulation jacket and must be designed to avoid thread or latch seizure in the adverse environment. High temperature lubricants used to prevent seal or latch seizures contaminate the reaction zone and the thermal radiation shields. An adequate vacuum is very difficult to maintain and the closure seals must be replaced each time the reactor is opened.

With the existing cold-seal design, there is no way for reactive gases to enter the vacuum jacket except through a weld or shell failure. This provides very consistent insulation performance. The cartridge is completely exposed and readily removable when the enclosing shell is removed. Every surface and passage of the reactor assembly can be readily exposed for inspection without destroying any component. This is especially important for heat exchanger maintenance until a heat exchanger material is found that is absolutely non-reactive. For example, even slow reactions in the inaccessible passages of compact heat exchangers designed for hot-seal units soon block the recycle flow or split a weld seam and a replacement is required. Slow reactions have been observed many times on the cold-seal heat exchanger surfaces and have been cleaned and treated with inhibiting materials with negligible program interruption. When a non-reactive material or treatment is found so that accessibility is not important, a more compact cold-seal unit will be possible.

3.5.3 Horizontal vs. Vertical Reactor Orientation. - The primary factors influencing choice of reactor orientation were simplicity of supporting the assembly and ease of exchanging cartridges. This resulted in a horizontal axis for the hot-seal unit where suitable shell support points were available and the cartridge could be more easily slid along its support shaft, then lifted vertically with the minimum grasping area available. The reactor and insulation jacket covers were also more conveniently manageable in the horizontal position.

The vertical axis of the cold-seal unit allowed the use of a counter-weight to assist in shell removal. With the shell removed, a full grasp of the cartridge was available for lifting it from the unit (Figure 3.13). Horizontal orientation would have required a rail system for jacket removal and cantilever support for the cartridge and inner heat exchanger shell.

3.5.4 Catalyst Zone Packing vs. Uniform Distribution. - It has been noted (Ref. 4) that the pressure differential buildup with accumulated metabolic load is appreciably lower if the reaction has been interrupted by a cooling and reheat period. This is presumably due to disruption of the carbon structure by thermally imposed stresses. Since process interruption is undesirable, several other methods of disrupting the carbon structure have been tried. With uniform steel wool distribution between the core and outer shell, the highest carbon density and hardest crust tends to form near the core where reaction equilibrium is least advanced. The higher density and lower area for flow in this zone cause more rapid flow restriction than if the same amount of carbon were deposited around the perimeter of the catalyst bed.

An effective way to assure maximum deposition in the outer zone is to pack the steel wool in this area, leaving the inner zone open. Any crust formation at the inner face of the catalyst muff is then disrupted as it is forced toward the core by the carbon being deposited between it and the outer shell. Eventually the inner zone is completely filled with relatively lightly packed carbon without excessive flow restriction. The carbon movement generated by this method also tends to break up flow channels and helps to prevent bypass flow between the carbon block and the cartridge ends.

3.5.5 Catalyst Support. - At a fixed reactor temperature and recycle gas composition, the lowest total power consumption occurs when the process rate is maintained with the least possible recycle flow. A decrease in recycle flow reduces both compressor and heater power but is most influential on the latter because for a given reactor environment and heat exchanger performance the energy delivered to the condenser is a direct function of the flow. Tests have shown that cartridges carefully packaged to eliminate catalyst slumping and flow channeling can be operated with less than 20 percent deviation in flow required for a given process rate. Flow channeling can easily double or triple the recycle flow requirement as the carbon compacts during the life of the cartridge. For these reasons, catalyst support has a very critical influence on power consumption.

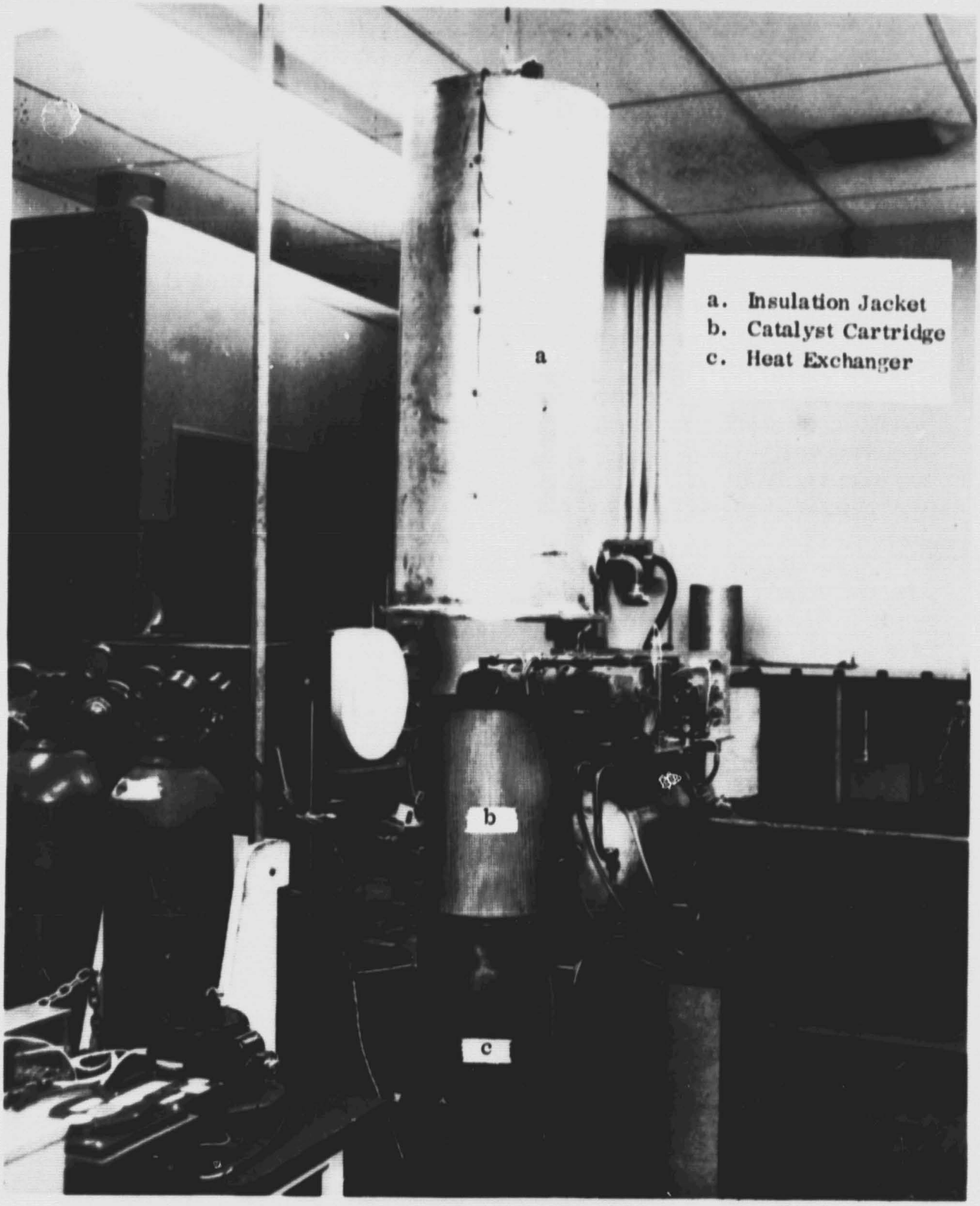

Figure 3.13 - Cold-Seal Unit

In the hot-seal units, the cartridges were positioned horizontally to simplify reactor cover removal and cartridge extraction and replacement. In operation during gravity conditions, the vertical dimensions of the steel wool catalyst muff were relatively small and slumping due to softening or deterioration of the strands was limited by the support provided by the cartridge core and lower half of the cartridge shell. Although no special supports were developed for this configuration, they would undoubtedly have improved reactor performance.

The cold-seal unit was positioned vertically to simplify removal of the shell and insulation jacket assembly for cartridge replacement. The vertical position exposed a 35.6 cm (14-inch) high column of catalyst to slumping forces and without support a 15.2 cm (6-inch) gap formed between the catalyst and cartridge top soon after reaction was initiated. Fortunately, this made development of a support system mandatory. The resulting improvement in performance and predictability are well worth the added effort in packaging. Although additional simplification and performance improvement concepts are being experimentally evaluated, the basic approach has been to provide sufficient vertical columns around the perimeter or core to prevent excessive sagging between columns.

The following packing procedure, illustrated in Figure 3.14, has produced effective cartridges. A reel of No. 3 steel wool ribbon is solvent degreased and air dried. Some of it may be further pretreated before being cut into lengths to form 20 cm (8-inch) O.D. rings. Enough rings are packed into the annular space between 10 and 20 cm (4 and 8-inch) diameter tubes 36 cm (14 inches) tall to provide 250 to 280 grams of catalyst. The outer tube is removed and channel-shaped wire mesh vertical supports are pressed into the outer surface. The inner form is then removed and wire ties are passed through the steel wool muff from the inside and fastened to the support channels. Three ties are used for each support. The cartridge core, base, and shell are assembled with their respective quartz fiber liners and the catalyst muff is placed inside. Before the cover is installed, a flat ring of wire mesh is placed on top of the muff with a small ring of steel wool above it to further discourage gaps at the cover end.

The number of supports has been varied from four external channels to six external and six internal channels. The best results to date have been obtained with six external and two internal supports. The supports are made from welded galvanized iron screen of 1.27 × 1.27 cm (1/2 × 1/2-inch) mesh from which the zinc is removed in an acid bath. Ladder-shaped strips are cut having two vertical wires and sufficient horizontal wire protrusions to bend into a channel with prongs to support the steel wool.

The space provided between the 10 cm (4-inch) inside diameter of the catalyst muff and the 4.45 cm (1.75-inch) diameter of the cartridge core gives the carbon

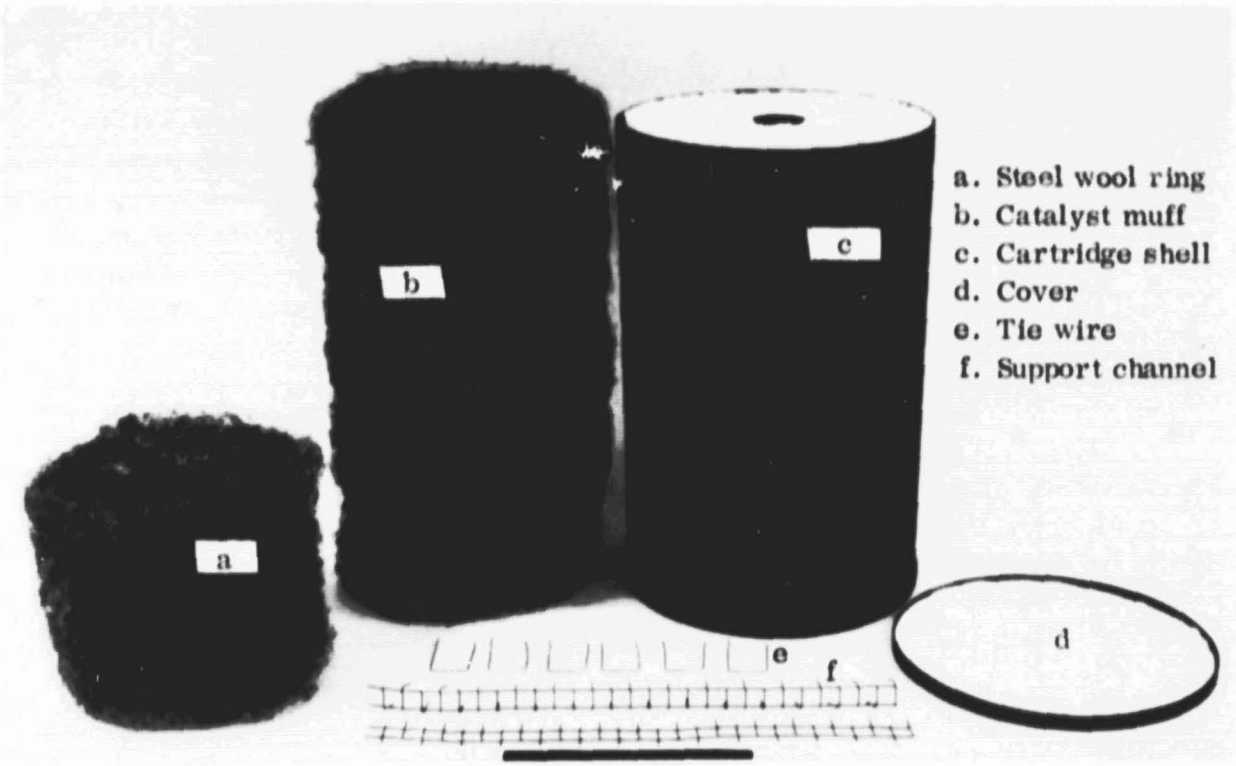

Figure 3.14 - Cartridge Components

block an opportunity to flow as growth pressures are generated. This prevents generation of dense surface crusts substantially reducing pressure differential build-up and extending cartridge life.

3.5.6 Recuperative Heat Exchangers. - The formed-convolution recuperative heat exchangers used in the final configuration of hot-seal independent units did not perform as well as expected. Conservative design calculations predicted temperature effectiveness values of 88 to 93 percent but operational data indicated a 78 to 83 percent range. The discrepancy could not be rationalized analytically except by assuming the heat exchanger passages were not of the specified dimensions. The most likely dimensional deviation was assumed to be in the convolution form. Heat exchanger X-rays subsequently confirmed that the convolutions were omega shaped rather than parallel walled as specified.

The concentric shell recuperative heat exchanger of the cold seal reactor was designed for 94 percent effectiveness and operational data show approximately 95 percent. Among explanations for the higher value are the probability that the gaps between the shells are at the low end of the design tolerance; the head and flange of the middle shell provide heat exchange surface not accounted for in design analysis; and heat loss through the heat exchanger insulation could cause an apparent increase in effectiveness.

3.5.7 Insulation Configurations. - Both the hot-seal and cold-seal reactor/heat exchanger assemblies were vacuum jacketed with multi-layered insulation and radiation shields for low insulation volume. This provides effective insulation when good vacuums are maintained and heat leakage through support members is minimized. Maintaining a good vacuum was especially difficult with hot-seal units because the adapter and large cartridge access area seals of the reactor were exposed to a reactive high temperature environment with a full pressure differential of working pressure plus vacuum. All resulting leakage went directly into the vacuum jacket. High temperature lubricants used to prevent seal bonding or thread seizures contaminated the reactor, recycle loop and thermal radiation shields. Except for the heater flange, all of the closures of the cold-seal unit are in a non-reactive low temperature environment.

The pressure differential across the cartridge access seal is from heat exchanger discharge pressure to atmospheric pressure with no communication to the vacuum jacket. This has provided very consistent insulation performance.

3.6 Materials Research

The most persistent problem associated with development of hardware for the Bosch process results from reactions between the hot recycle gases and material surfaces outside of the catalyst bed. These reactions may adversely affect the structural characteristics of the material or cause carbon to form where it is not wanted. The rate of reaction and area of the reactive site often increase and spread with operating time depending primarily on the type of material and its surface condition. The general approach toward eliminating or minimizing this problem has been to: (1) study the thermodynamics of chemical interactions between the reactive gas mixture and various materials; (2) evaluate materials by exposing test specimens to the reactive environment; (3) evaluate construction materials experience; and (4) assess the results of reaction inhibiting surface treatments.

Observations concerning the effects of catalyst activating treatments and system contaminants on starting and operational characteristics are also included in this section.

3.6.1 Construction Materials Experience. - Electroless nickel plated 300 series stainless steels and Incoloy 800 have been used in several reactor applications. The effectiveness of electroless nickel has been assumed to be due to the relatively non-porous barrier it provides compared to electrolytic plating and its high phosphorus content which acts to inhibit catalytic action. The prototype unit (Ref. 4) successfully used electroless nickel to protect the stainless steel cartridge components, reactor cover plates, and heater sheath. Contrary to this experience, the electroless nickel plating on the hot-seal advanced unit reactor shells, cover plates,

and heater sheath gradually deteriorated and catalytic carbon formed on the exposed substrate. This unexpected performance may be due to the change in plating conditions occasioned by the larger components involved. Previously, components were plated in solutions that were discarded after each use. The advanced unit components were plated in a bath that was kept in use by replenishing the chemicals necessary to maintain the proper plating concentrations.

Aluminide coated stainless steel parts have been used in several applications. The coating has been applied to salvage a reactor shell but normally was used on new components. Aluminide coatings on new components have been generally non-reactive. The surface tends to darken with exposure and occasionally a local spot may show signs of carbon formation. No rapid growth or spread has been observed. No appreciable deterioration of aluminided Incoloy 800 heater sheaths has been noticed. After failure of the electroless nickel plating in some areas of the advanced unit reactor shell, the surface was stripped with nitric acid and vapor honed to remove all plating and carbon deposits. The shell was then coated with the same type of aluminide material used successfully on cartridge parts. This treatment was not effective in protecting the areas that were previously active.

With the exceptions of the aluminide-coated heater sheath and cartridge components, the high temperature areas of the cold-seal reactor were fabricated from Inconel 718. After construction, the Inconel 718 surfaces were vapor honed to remove contaminants and weld discoloration.

Limited areas of the heated Inconel 718 surfaces darkened during the first few runs and in about 400 hours a small spot had developed a slow carbon depositing reaction. The area of this spot slowly increased and appeared to progress more rapidly along hand weld seams. Machine weld seams did not appear to be any more susceptible to reaction than the adjacent surfaces.

Several approaches were used to stop carbon formation on the Inconel 718 shells. Vapor honing the surface to remove carbon deposits and contaminants was not effective. A coating of dry film lubricant containing molybdenum disulfide temporarily inhibited surface reactions but also poisoned the steel wool catalyst making reaction starts unpredictable. Circulating a mixture of sulfur dioxide and air through the hot reactor effectively inhibited surface reactions for a short while but residual contamination also affected the starting properties of the steel wool catalyst. Rubbing the surface with a bar of tin/lead solder was found to stop carbon deposition. Controlled tests indicated that lead was the effective agent so selected areas were painted with a mixture of red lead oxide and glycerine. This treatment has been quite effective for the 600 hours of operation since the first area was treated. Massive applications can adversely influence the catalyst for a subsequent run or two, indicating that lead vapor diffuses throughout the reactor.

The progressive change of the Inconel 718 from inactive to moderately catalytic was not indicated by previous specimen exposure test. Initiation in weld areas may be due to detrimental changes in the chemical composition or metallurgical microstructure. Inconel 718 contains approximately 18 percent iron which at exposed surfaces may be converted to the active cementite form. Some of the iron in cementite may be replaced by manganese or nickel to make additional catalytic material available.

3.6.2 Specimen Exposure Tests. - Small specimens of candidate materials were placed in a cylindrical graphite felt pocket in the cartridge core. This exposed them to the most reactive gas compositions and highest reaction temperatures. All metal specimens were initially vapor honed to remove loose surface contaminants. The weight and surface area of each specimen was measured before the initial exposure. Surface areas varied from 1 to 15 cm^2. Prior to microscopic examinations and weighings between runs, the specimens were cleaned by ultrasonic agitation in 1.1.1-trichloroethane to remove loose materials. Specimen data and observations are presented in Table 3.2 with amplification in the following discussion.

Specimens of constantan and Monel were the only ones to form rather thick adherent coats of carbon and degraded material. Both had relatively large weight increases during each exposure period.

Many of the metal specimens formed carbon in small active sites. During the ultrasonic cleaning of these specimens, the carbon and degraded metal were removed leaving small craters or pits. Gradual weight losses were recorded for repeated exposures. Some materials pitted on all surfaces while others pitted only on mill rolled faces suggesting surface contamination or processing inhomogeneity.

Other metal specimens showed no evidence of catalytic carbon formation, pitting or significant weight change although some were discolored by exposure to the reactive environment. This group, composed of Inconel 625, Inconel 671, NA 64, More 2, and Tungsten, merits further evaluation. A platinum specimen remained bright and free of carbon deposits but showed a significant weight increase analytically determined to be caused by zinc accretion. The source of zinc was apparently due to incomplete stripping of the galvanized support channels.

The ceramic materials, Mullite and alumina, appeared to be non-catalytic and unaffected by exposure to the reactive environment.

3.6.3 Thermodynamic Stability of Metal Carbides. - In an effort to predict the behavior of metals and their alloying elements in an operating Bosch environment, the free energy of formation values of several metallic carbides were calculated and are plotted as a function of temperature in Figure 3.15. Negative values of free energy correspond with carbide-forming reactions that are exothermic. The relative

TABLE 3.2 - MATERIALS EXPOSURE SPECIMENS

Material	Nominal Chemical Composition Major Alloying Elements (%)								Weight Change	Bosch Exposure	Remarks
	Mn	Cr	Ni	Fe	Co	Mo	Cb	W	(mg/cm^2)	(Hr)	
Alumina	(99% Al_2O_3)								-0.02	1534	No detrimental reactions appear to have occurred. Some carbon adhered to the surface that was not removed by ultrasonic cleaning.
Constantan			40			(Cu Rem)			+1.96	1196	A surface coating was formed. Material was degrading and carbon was forming.
Hastelloy X	.5	22	Bal	18	1.5	9	-	.6	-0.11	607	Many reaction sites, pits, on surface.
Haynes 6B	1	30	2	2	Bal	1	-	4.5	-0.32	221	Surface generally covered with small reaction pits. Edges appear less reactive than the mill finish surface.
Haynes 188	.75	22	22	1.5	Bal	-	-	14	-0.14	607	Many reaction sites, pits, on surface. Some pits connected in a line as a surface scratch or contamination. Sheared edges less reactive.
Inconel 601	.5	23	61	14		(Al 1.3)			-0.16	607	Surface lightly pitted with reaction sites.
Inconel 625	.2	22	61	3	-	9	3.6	-	-0.03	1916	Surface darkened. No evidence of catalytic carbon formation or pitting.
Inconel 671	-	50	50	-	-	-	-	-	+0.14	1916	Surface darkened. No evidence of catalytic carbon formation or pitting.
Inconel 702	.1	15	79	.4		(Ti .6) (Al 3.2)			-0.46	221	Surface generally covered with reaction pits. Sheared edges appear less reactive than the rolled surfaces.
Inconel 718	.2	19	52 (Ti 0.9,	18 Al 0.5)	-	3	5.3	-	+0.03	1916	Some reactive sites appear to have developed on one side. All other surfaces darkened but no pitting or catalytic carbon formations.
Incoloy 800	.8	21	32 (Ti 0.4,	46 Al 0.4)	-	-	-	-	-1.49	353	Many small reaction pits. Reaction pits also on sheared edges.
Monel			65			(Cu Rem)			+8.89	239	Surface coated with a rather thick black film. Not a pitting type reaction. Specimen not embrittled.
More 2	.2	34	50	-	-	-	-	16	+0.14	1058	Surface darkened. No pits, films or catalytic carbon were formed.
Mullite									-0.23	1534	Carbon adhered to surface from contact with carbon in reactor. Weight loss due to particles breaking off specimen.
NA 64	-	60	40	-	-	-	-	-	+0.36	1534	Surface darkened. No pits, films, or catalytic carbon were formed.
Platinum	(Pt 99.9+)								+1.03	1534	Surface remained bright but metal grain size became larger and accented. Weight gain appeared due to Zn and W.
Silicon carbide	(SiC, Heating Element)									1058	Original material was granular. Exposure weakened bonds between granules and material crumbled quite easily.
Stainless Steel Type 310	1	25	20	Bal	-	-	-	-	-0.67	1916	Some reaction started on sharp corners. A few spots on the surface appeared reactive.
Stainless Steel Type 347	1	18	11	Bal	-	-	1	-	-1.39	353	Many small reaction pits. Reaction pits also on sheared edges.
Stainless Steel 22-13-5	5	22	13	Bal	-	-	-	-	-0.08	221	Catalytic reaction and material degradation on sharp edges. Some reaction craters formed on the rolled surface.
Tungsten	-	-	-	-	-	-	-	100	-0.32	1534	Surface was darkened. No catalytic carbon formed.
Zirconium Silicate Ceramic									+0.54	1534	Surface was quite porous-looking. This resulted in carbon pickup from other sources. No reaction or degradation observed.
RA 333	1.5	25 (Si 1.2)	Bal	18	3	3	-	3	-0.03	353	Surface lightly covered with small craters of reaction. No reaction pits observed on sawed and filed edges.

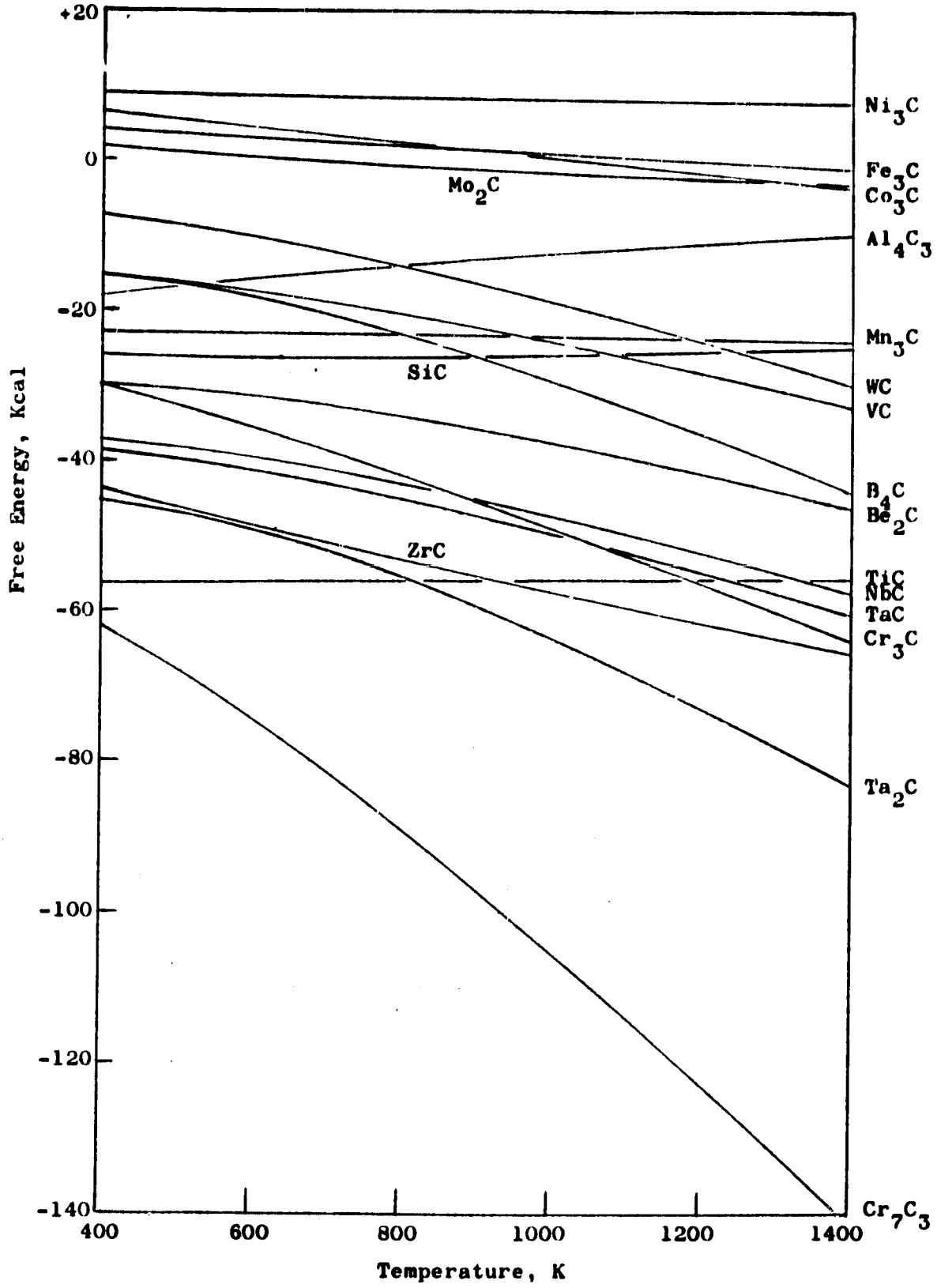

Figure 3.15 - Free Energy of Formation of Metal Carbides

thermodynamic stability of the carbides may be found by comparing values of free energy at any temperature of interest, the carbide with the lower free energy of formation being the more stable. Thus, at 900 K, Cr_7C_3 is more stable than TiC, and TiC is more stable than Co_3C. Reference 12 was the source of the thermodynamic relationships used for the calculations, and several other data sources were used.

The relative free energies of formation may be used to estimate the manner in which the two or more metals of an alloy will react with carburizing gases. For example, Figure 3.15 shows that the free energy change in the formation of iron, nickel, cobalt, and molybdenum carbides is quite small (i.e., nearer zero) compared with that of chromium, tantalum, and niobium. This means that the driving force for the formation of chromium carbide on the surface of a chromium-containing alloy in a carburizing atmosphere such as exists in the Bosch reactor at 900 K (1600 F) is much greater than the force for the formation of iron or nickel carbides. The formation of a thermodynamically stable chromium carbide layer on the surface of an alloy should protect other alloying metals such as iron and nickel from carbide-forming reactions if there is no mechanical rupture of the surface due to volume change in formation of the chromium carbide. Most metal carbides are less dense than the parent metal and should cause some compressive stress during formation. Exceptions are silicon, zirconium, and titanium where little volume change is associated with carbide formation.

Tantalum, niobium, titanium, zirconium, silicon, boron, beryllium, vanadium, tungsten, and manganese are other metals having negative free energies of carbide formation at 900 K. Of these, niobium, titanium, silicon, and tungsten as well as chromium, are used as alloying elements in commercially available alloys for resisting reactions with high temperature carburizing atmospheres.

Another way of portraying the relative activity of carbon in various metal carbides is shown in Figure 3.16. Here the ordinate is a ratio of carbon activity in the carbide to the activity of graphite (standard state). These ratios can be used to estimate the equilibrium sharing of carbon as carbides in alloys of two or more metals. From Figure 3.16, it can be seen that the activity of carbon at 900 K in titanium carbide or niobium carbide is much less than that in chromium carbide or iron carbide. This results in preferential formation of titanium carbide or niobium carbide until the available titanium or niobium metal has reacted.

Figures 3.15 and 3.16 also show similarity in the thermodynamic properties of iron and cobalt carbides. Both appear to be thermodynamically unstable in the 900 to 1000 K range. This has been observed experimentally where both cobalt metal and cobalt alloys have behaved catalytically in the operating Bosch environment similar to iron and iron alloys. Nickel carbide lies above both the iron and cobalt carbide curves. This would allow one to predict that the formation of nickel carbide

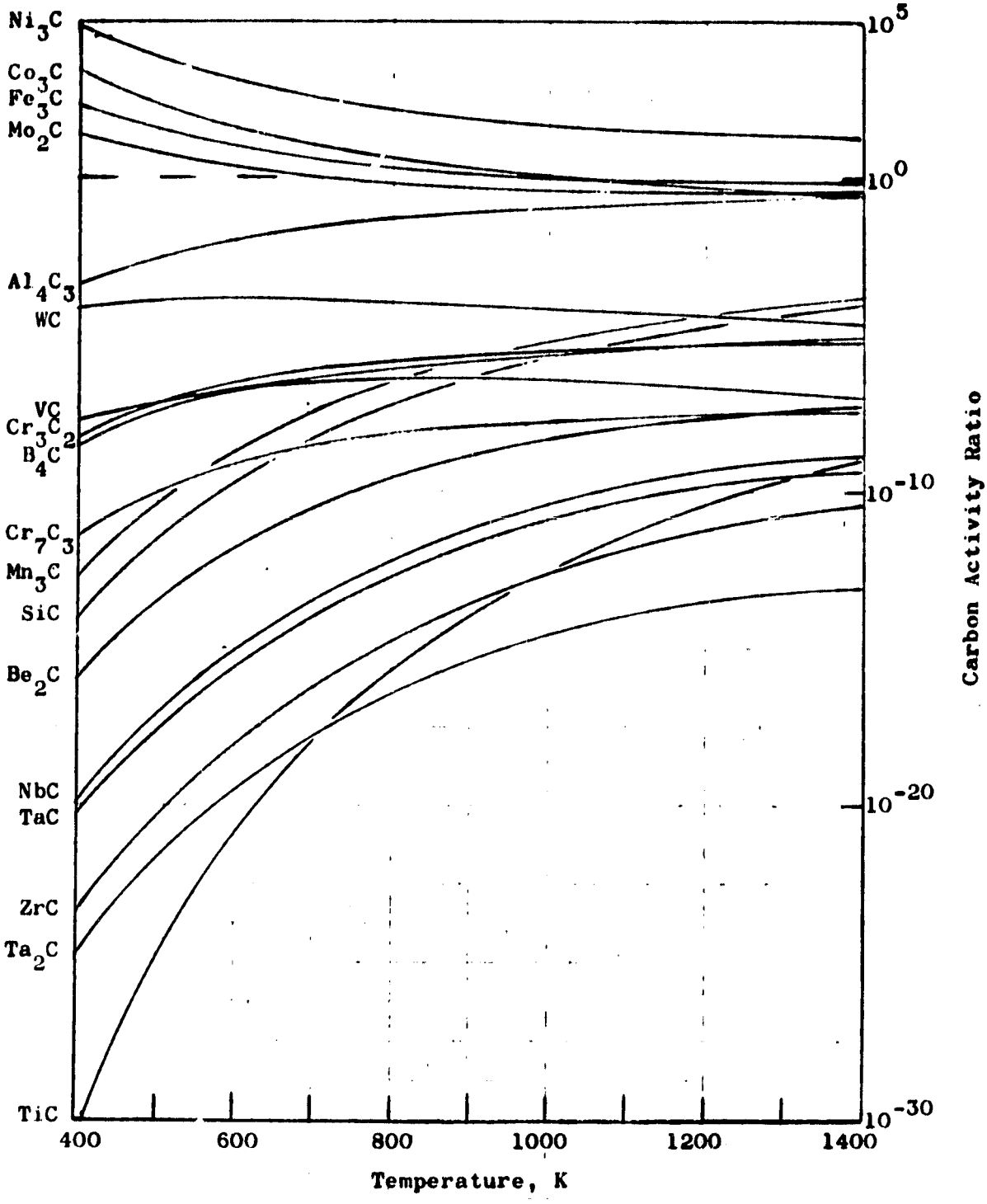

Figure 3.16 - Carbon Activity Ratio of Metal Carbides

would be more difficult than the formation of iron or cobalt carbides. Molybdenum carbide lies slightly below iron, cobalt, and nickel carbides. One might predict that molybdenum carbide would be relatively unstable and might behave catalytically. No such carbon forming reactions have been observed in our exposures of molybdenum metal. Molybdenum metal was severely embrittled by Bosch reactor exposure, probably due to reaction with hydrogen in the recycle gas. Other metals which react and degrade with hydrogen in the Bosch reactor are titanium and zirconium.

The formation of tungsten carbide from tungsten metal during Bosch reactor exposure might be predicted from Figure 3.15. However, Bosch reactor exposure of tungsten did not result in a weight gain as would be expected from carbide formation. The tungsten lost some weight and was embrittled by the exposure and this might be attributed to volatile oxide formation or hydrogen reactions.

The conclusions which may be drawn from this study are that metals which form no carbides, such as copper or platinum, would be preferred for Bosch reactor construction if non-reactivity were the only consideration. Since cost, mechanical properties, and thermal properties are of considerable importance, a nickel base alloy holds the most promise of being non-catalytic and non-embrittled by Bosch reactor exposure. All of the other metals investigated are catalytic, form carbides readily, or are embrittled by hydrogen exposure. The alloying elements in the nickel alloy must not be catalytic, which eliminates iron and cobalt. The alloying elements should be in sufficient concentration to provide an adherent protective film on the surface of the alloy to prevent diffusion of gases and carbon into the interior of the alloy. The protective film could be either a carbide or a not easily reduced oxide. In addition, the alloying element, if present in large quantity, must not react with hydrogen since hydrogen could diffuse through the alloy and embrittle it. These restrictions limit the alloying to elements such as chromium and silicon.

3.6.4 Catalyst Conditioning. - The purpose of steel wool catalyst conditioning is to obtain prompt and reliable starting characteristics with consistent cartridge life and minimum product water pollution. Treatments that excessively deteriorate the steel wool fiber cause support problems and encourage flow channeling that adversely affects cartridge life. Starts have been made with "as received" steel wool but the starting time is inconsistent and cutting oil or preservative residues contaminate the product water. Therefore, minimum conditioning is considered to be a thorough vapor degreasing with 1.1.1-trichloroethane.

An additional surface treatment greatly improves the starting reliability, especially when a source of catalyst contaminant exists. This treatment consists of immersing the degreased steel wool in a 2 percent (vol) hydrochloric acid solution for one minute followed by a water rinse, brisk shaking to remove excess water, and oven drying at 420 K (300 F) for about 15 minutes. The etching process removes

some surface contaminants, increases the surface area, and forms a light rust on the surface. Fiber deterioration is very mild and is usually compensated for by mixing etched and unetched batches of steel wool during the cartridge packing procedure. Starts to a process rate at a 4-man level in 1.5 to 2.0 hours are consistently obtained if abnormal conditions are not imposed.

4.0 CONCLUSIONS

The work of this contract period brought significant advances in all areas of concern and narrowed the list of non-reactive materials structurally suitable for high temperature components of the Bosch unit. The following conclusions are based on recent achievements:

1. The cold-seal reactor configuration is superior to any of the preceding hot-seal configurations, notably in: (a) better access to the cartridge for removal and replacement; (b) less gas leakage due to better seal environment; (c) excellent access to formerly inaccessible high-temperature surfaces enabling inspection, cleaning and other maintenance; (d) better insulation performance through simplified packaging and better vacuum seal conditions; and (e) better heat exchanger performance with design simplicity, easy fabrication, and high effectiveness.

2. The measured heat exchanger temperature effectiveness (about 95 percent) exceeded effectiveness predicted by heat transfer calculations (about 94 percent), and is near the feasible maximum. Any further effectiveness gains will be relatively hard to achieve.

3. Temperatures, pressures, mixture compositions, and other parameters for successful operation are well defined and their optimum values are not highly critical. Optimum parameter relationships for minimum power consumption have been closely approached but ultimate values have not been established because of limitations of the present mixture control unit.

4. In comparing three methods of process rate control, the back pressure regulator formerly used is considered obsolete because it imposes a substantial parasitic power load. The compressor bypass mode is preferred when the process load is relatively constant because its parasitic power load is quite small. The relatively complex variable compressor speed mode shows minimum power requirements during much of the life of a cartridge. The savings might justify this mode if the process rate must be variable over a large range, e.g., from 4- to 8-man metabolic loads.

5. The design and fabrication techniques for the high-temperature vacuum insulation jacket gave fairly good performance. Small additional gains are probably attainable.

6. The configuration of two independent reactor units is preferable to the former dual reactor units sharing one set of controls and recycle components, for reasons of lower operating power, higher reliability, and simplicity of cartridge change operations.

7. Correct catalyst preparation and packing techniques are known and are very important to efficient operation. Improper catalyst support allows flow channeling and results in substantially higher power consumption. This factor far exceeds influences of moderate variations in temperatures or mixture composition, and may be severe enough that the intended process rate cannot be maintained.

Except for materials selection, Bosch unit development is approaching a level of maturity consistent with expectations for ground-based operation. Intensive effort on the materials problem is recommended. Assuming satisfactory progress in this area, the next step could be development of a flight prototype.

5.0 REFERENCES

1. Armstrong, R. C., et al. Life Support System for Space Flights of Extended Time Periods, NASA CR-614, Convair division of General Dynamics, San Diego, Calif., November 1966.

2. North, B. F. NASA/Langley Integrated Life Support System Program Summary for the Period February 1966 Through August 1967, Report GDC-DBD67-003, Convair division of General Dynamics, San Diego, Calif., November 1967.

3. Pecoraro, J. N., Pearson, A. O., Drake, G. L., and Burnett, J.R. Contribution of a Developmental Integrated Life Support System to Aerospace Technology, AIAA 4th Annual Meeting and Technical Display, No. 67-924, October 1967.

4. Holmes, R. F., Keller, E. E., and King, C. D. A Carbon Dioxide Reduction Unit Using Bosch Reaction and Expendable Catalyst Cartridges, NASA CR-1682, Convair division of General Dynamics, San Diego, Calif., November 1970.

5. King, C. D., and Holmes, R. F. Design and Fabrication of a Carbon Dioxide Unit for Oxygen Recovery in a Life Support System, Report GDC-ERR-1400, Convair division of General Dynamics, San Diego, Calif., December 1969.

6. Holmes, R. F. Operational Characteristics of a Research Carbon Dioxide Reduction Unit for Oxygen Recovery in a Life Support System. Report GDC-ERR-1522, Convair division of General Dynamics, San Diego, Calif., October 1970.

7. King, C. D., Holmes, R. F., and Keller, E. E. Design Optimization Studies for CO_2 Reduction by the Bosch Process, Report GDC-ERR-1658, Convair division of General Dynamics, San Diego, Calif., 15 December 1971.

8. Holmes, R. F., King, C. D., and Keller, E. E. Bosch CO_2 Reduction System Development, Report GDC-DBD73-001, Convair Aerospace division of General Dynamics, San Diego, Calif., 1973.

9. Holmes, R. F., North, B. F., Keller, E. E., and Russ, E. J. Bosch CO_2 Reduction System Development Interim Report No. 2, Report CASD-NAS-74-018, Convair division of General Dynamics, San Diego, Calif., 1974.

10. King, C. D., Russ, E. J., Girouard, H. D., and Chiarappa, D. J. Oxygen Regeneration/Reaction Control Systems Concept Study, Report GDCA-DBD73-003, Convair Aerospace division of General Dynamics, San Diego, Calif., 1972.

11. Giedt, W. H. Principles of Engineering Heat Transfer, Van Nostrand, 1957.

12. Darken, L. S., et al. Physical Chemistry of Metals, Chapter 14, McGraw-Hill Book Co., Inc., New York, 1953.